AD-A042 219 NAVAL RESEARCH LAB WASHINGTON D C F/G 11/6
STRUCTURAL INTEGRITY OF WATER REACTOR PRESSURE BOUNDARY COMPONE--ETC(U)
MAY 77 F J LOSS AT(49-24)-0207
UNCLASSIFIED NRL/NUREG-MR-3512 NL

| OF |

AD
A042219

END

DATE
FILMED
8-77

(12)

NRL/NUREG Memorandum Report 3512

Structural Integrity of Water Reactor Pressure Boundary Components
Progress Report Ending 28 February 1977

F. J. Loss, *Editor*

Thermostructural Materials Branch
Engineering Materials Division

May 1977

Prepared for the U.S. Nuclear Regulatory Commission,
Office of Nuclear Regulatory Research under Contract
AT(49-24)-0207

NAVAL RESEARCH LABORATORY
Washington, D.C.

Distribution: NRC-1 and NRC-5

SECURITY CLASSIFICATION OF THIS PAGE (When Data Entered)

REPORT DOCUMENTATION PAGE		READ INSTRUCTIONS BEFORE COMPLETING FORM
1. REPORT NUMBER NRL/NUREG Memorandum Report 3512	2. GOVT ACCESSION NO.	3. RECIPIENT'S CATALOG NUMBER
4. TITLE (and Subtitle) (6) STRUCTURAL INTEGRITY OF WATER REACTOR PRESSURE BOUNDARY COMPONENTS.		5. TYPE OF REPORT & PERIOD COVERED Interim report on a continuing NRL problem.
		6. PERFORMING ORG. REPORT NUMBER
7. AUTHOR(s) (10) F. J. Loss, Editor		8. CONTRACT OR GRANT NUMBER(s)
9. PERFORMING ORGANIZATION NAME AND ADDRESS Naval Research Laboratory Washington, D.C. 20375		10. PROGRAM ELEMENT, PROJECT, TASK AREA & WORK UNIT NUMBERS NRL Problem M01-40 (15) Project AT(49-24)-0207
11. CONTROLLING OFFICE NAME AND ADDRESS U.S. Nuclear Regulatory Commission Division of Reactor Safety Research Washington, D.C. 20555		12. REPORT DATE (11) May 1977
		13. NUMBER OF PAGES 56
14. MONITORING AGENCY NAME & ADDRESS(if different from Controlling Office) (9) Progress rept. for period ending 28 Feb 77,		15. SECURITY CLASS. (of this report) UNCLASSIFIED
		15a. DECLASSIFICATION/DOWNGRADING SCHEDULE
16. DISTRIBUTION STATEMENT (of this Report) Approved for public release; distribution unlimited. (12) 58p. (14) NRL/NUREG-MR-3512		
17. DISTRIBUTION STATEMENT (of the abstract entered in Block 20, if different from Report)		
18. SUPPLEMENTARY NOTES Prepared for the U.S. Nuclear Regulatory Commission, Office of Nuclear Regulatory Research under Contract AT(49-24)-0207		
19. KEY WORDS (Continue on reverse side if necessary and identify by block number) Nuclear pressure vessel steels; Warm prestress; Thermal shock; Charpy-V test; Radiation sensitivity; Postirradiation recovery; Residual impurities; Fatigue crack propagation; Vessel integrity		

20. ABSTRACT (Continue on reverse side if necessary and identify by block number)

This report describes research progress in a continuing program to characterize materials properties performance with respect to structural integrity of light water reactor pressure boundary components. Progress for this reporting period is summarized in the following areas:

(a) Radiation embrittlement resistance of A533-B Class 1 steel plate as a function of extra low copper impurity content

(b) Influence of phosphorus and copper content on post-irradiation upper shelf toughness and

(Continues) over

DD FORM 1 JAN 73 1473 EDITION OF 1 NOV 65 IS OBSOLETE S/N 0102-014-6601

SECURITY CLASSIFICATION OF THIS PAGE (When Data Entered)

251950

LB

20. Abstract (Continued)

postirradiation toughness recovery for A533-B steel plate and weld metal
(c) Investigations of warm prestress and plastic net ligament phenomena as a means to mitigate crack extension in a vessel during a loss of coolant accident
(d) Evaluation of critical factors in crack growth rate studies in a pressurized water reactor environment.

CONTENTS

STRUCTURAL INTEGRITY OF WATER REACTOR
PRESSURE BOUNDARY COMPONENTS

PROGRESS REPORT ENDING 28 FEBRUARY 1977

SUMMARY

I. RADIATION SENSITIVITY AND POSTIRRADIATION PROPERTIES RECOVERY

A. NRC-CE-NRL Cooperative Program: Series 3 (Extra Low Copper) Material Evaluations

Preliminary radiation assessments of notch ductility for the Series 3 materials (extra low copper content) from the NRC-CE-NRL Cooperative Program have been completed. The materials represent best current steelmaking practice and copper impurity control. These primary observations were made from the results in conjunction with determinations for Series 2 (low copper content) and Series 1 (normal copper content, nonimproved steelmaking practice) materials. First, the specification of 0.06% Cu maximum as opposed to 0.10% Cu maximum does not provide a large beneficial increase in 288°C (550°F) radiation resistance for A533-B steel for the fluence range investigated. Second, all Series 3 materials (plate, weld, and weld heat affected zone) exhibited very high radiation resistance wherein brittle/ductile transition evaluations were less than 56°C (100°F) for fluences of ~$5x10^{19}$ n/cm^2. Finally, the weld deposit demonstrated that nickel contents in amounts up to 1% do not contribute separately to radiation effects sensitivity in low copper content A533 welds. A final report on this phase of the cooperative program is in preparation.

B. Influence of Phosphorus and Copper on Postirradiation Upper Shelf Performance

An exploratory study has been made on the individual contributions of copper and phosphorus to upper shelf behavior with 288°C (550°F) irradiation and with 343 and 371°C (650 and 700°F) postirradiation annealing. Four A302-B and A533-B steel materials were employed. Fracture toughness determinations (K_{Jd}) as well as standard Charpy-V notch ductility determinations were made.

Note: Manuscript submitted April 28, 1977.

PRECEDING PAGE BLANK-NOT FILMED

Assessments of copper and phosphorus effects for the as-irradiated condition were not conclusive but do suggest a role of these impurities in upper shelf degradation. For the postirradiation annealed condition, the data demonstrate that upper shelf recovery decreases with increasing copper content. The findings also demonstrate that a difference of only 28°C (50°F) in annealing temperature (i.e., 371 vs 343°C, 700 vs 650°F) can have a very marked effect on upper shelf recovery.

II. THERMAL SHOCK-RELATED INVESTIGATIONS

A. Characterization of the Warm Prestress Phenomenon

An experimental study has been conducted to investigate the potential elevation in K_{Ic} by warm prestress (WPS) and to translate the significance of this behavior into structural terms in the sense of minimizing crack extension in nuclear vessel during a loss of coolant accident (LOCA). It is concluded that the mechanisms associated with WPS act to elevate the K_{Ic} of the material at the crack tip and that this fact can greatly minimize crack extension that would have been predicted without consideration of WPS. The experiments demonstrated that specimen fracture never occurs during the unloading portion of the simulated LOCA path. This finding is of major significance to the vessel integrity. Specifically, it implies that crack initiation in a vessel will not occur as K_I decreases with time regardless of the magnitude of K_{Ic}.

In terms of margin of safety against fracture, it is shown that the elevation of K_{Ic} by WPS is not uniform and depends upon WPS level, the degree of unloading, and the increment between the temperature of WPS and the failure temperature. In terms of structural significance, it is clear that WPS by itself cannot prevent the initiation of shallow cracks. For the typical vessel geometry considered, however, it is concluded that all cracks having relative initial depths greater than 0.2 are prevented, by WPS, from extending any amount. Finally, because of complete wall penetration during a LOCA predicted by a conservative elastic analysis without consideration of WPS, this phenomenon may form a key element upon which to predicate structural integrity during the accident.

B. Plastic Net Ligament Studies

A simulation of the plastic net ligament behavior associated with a deep, axial crack in a vessel wall during a LOCA was achieved. Using fatigue-cracked bend specimens, it was demonstrated that the bending of the vessel wall, due to

the thermal stresses, can result in neglibible crack extension of a deep crack; consequently, the vessel integrity will be maintained. This fact will prevent the loss of cooling water through the cracked wall and thereby preclude core melt down. The experiments were conducted with A533-B1 steel within the upper shelf toughness regime. Additional experiments are required to simulate the behavior of the wall when the temperature of the crack-tip region falls within the brittle-ductile transition region.

III. FATIGUE CRACK PROPAGATION IN LWR MATERIALS

A. Evaluation of Critical Factors in Crack Growth Rate Studies

Fatigue crack propagation data are presented for A508-2 forging material. Tests were conducted in accordance with the preliminary NRC matrix designed to characterize hydro and leak transients as well as heatup and cooldown transients of a commercial nuclear pressure vessel. To investigate the preceding transients, tests were conducted in 93°C (200°F) reactor grade water at atmospheric pressure and in 288°C (550°F) water at 14 MPa (2000 psig). A modified trapezoidal loading wave was used with a rapid rise time wherein the effect of hold time was investigated. The data show that hold times of 1, 3, and 12 minutes do not result in different growth rate trends at 93°C. Furthermore, the growth rates in 93°C water are essentially identical to those in an air environment; the behavior suggests that there is no effect of the water environment for the test conditions and material investigated.

RESEARCH PROGRESS

I. RADIATION SENSITIVITY AND POSTIRRADIATION PROPERTIES RECOVERY

A. NRC-CE-NRL Cooperative Program: Series 3 (Extra Low Copper) Material Evaluations

J. R. Hawthorne

BACKGROUND

The primary objective of the NRC-CE-NRL Cooperative Program on improved A533-B steel is to establish trends in radiation embrittlement resistance for three series of materials representing progressive reductions in allowable copper content. Each material series includes plates, weld deposits, and weld heat affected zone (HAZ) materials. The program builds on the findings of laboratory melt studies[1] which revealed that certain residual impurity elements, especially copper and phosphorus, have a particularly adverse effect on radiation resistance at reactor vessel service temperatures $\sim$288°C ($\sim$550°F). Conversely, the reduction of impurities was shown to yield steel with high radiation resistance. Demonstration tests with a commercial scale A533-B melt and weld[2,3] confirmed the conclusions based upon laboratory melts.

Materials in the present study were:

- Series 1 - normal copper content (> 0.15% Cu) typical of nonimproved commercial steel production (pre-1971).
- Series 2 - low copper content (0.10% Cu maximum with 0.012% P maximum) representing improved steel production (current practice).
- Series 3 - extra low copper content (0.06% Cu maximum) considered the practical lower limit for copper content control.

Findings for the Series 1 vs Series 2 materials have been reported.[4] The results clearly demonstrate that a major reduction in radiation sensitivity is achieved with reduced copper content in commercial production A533 plate, weld, and weld HAZ materials. The improvement was evident both as a smaller Charpy-V (C_V) transition temperature increase

(Fig. 1) and as a smaller decrease in C_V upper shelf energy level with irradiation.

A specific objective of the Series 3 vs Series 2 material assessments was to establish whether or not an additional benefit to radiation resistance is achieved by a very low copper content (optimum steelmaking practice) compared to a low copper content (improved practice only). During this reporting period, radiation assessments of the Series 3 materials were completed and permit this determination to be made.

MATERIALS

The chemical compositions of the Series 3 materials are given in Table 1 along with those for the Series 2 reference materials. It is noted that the Series 3 weld deposit was produced by the shielded metal arc (SMA) process whereas the Series 2 (and Series 1) welds were made by the submerged arc (S/A) process.[4] Welding parameters and materials used for the SMA weld are reported in Table 2. All welds for the program were produced using standard commercial equipment and practices.

The C_V specimens were taken from the quarter thickness locations of the plates in two orientations: longitudinal (LT, parallel to the plate primary rolling direction), and transverse (TL, perpendicular to the plate primary rolling direction). With one exception, only the TL orientation was evaluated with irradiation. Weld metal C_V specimens were removed between the 1/8 and 7/8 thickness locations and were oriented perpendicular to the welding direction. The HAZ C_V specimens were also oriented perpendicular to the welding direction but had the specimen V-notch centered 0.8mm (1/32 in.) in from the weld fusion line. The HAZ specimens correspond to the LT orientation, quarter thickness location, of the parent plate. In each case, the specimen notch was perpendicular to the plate (or weldment) surface. Drop weight test specimens (ASTM Type P-3) for unirradiated condition NDT determinations were taken either at the quarter thickness location (plate) or through the thickness (weld deposit).

MATERIAL IRRADIATIONS

Material irradiations were conducted in the Union Carbide Research Reactor (UCRR) D-3 fuel lattice position and in the University of Buffalo Reactor (UB) B-4 fuel lattice position. Target fluence levels* called for by the original program

*ϕ_{cs} - calculated spectrum fluence.
ϕ_{fs} - fission spectrum (assumed) fluence.

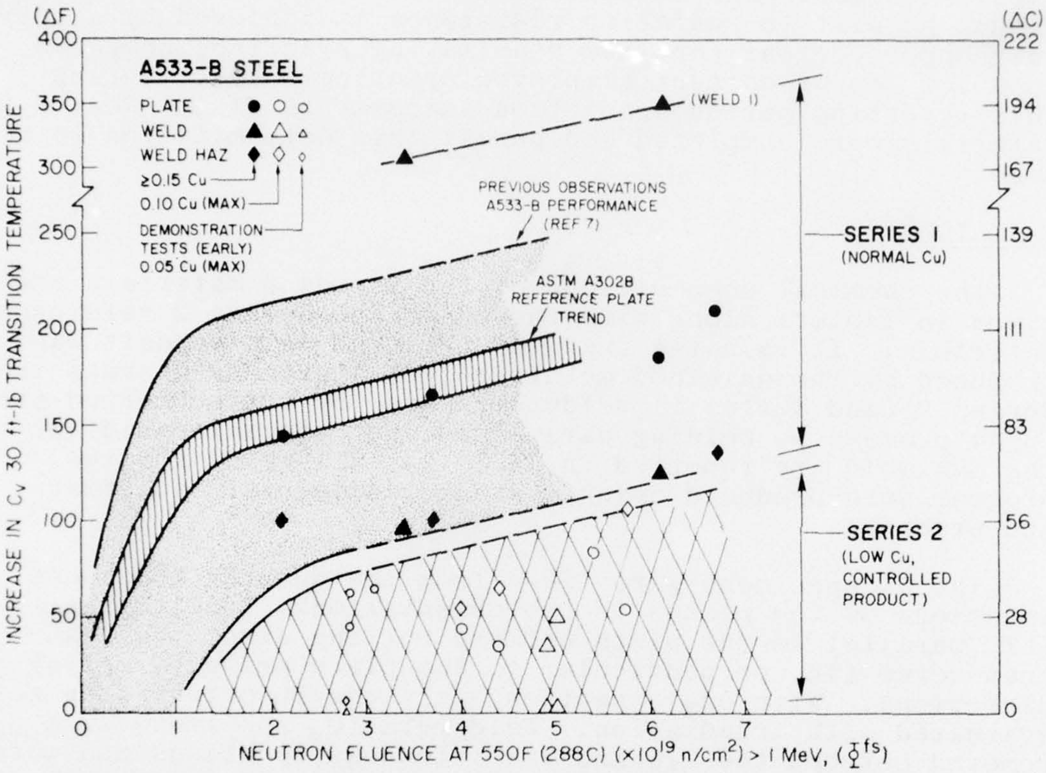

Fig. 1 — Summary of Charpy-V 40.7J (30 ft-lb) transition temperature changes with irradiation observed for Series 1 materials (large filled symbols) and Series 2 materials (large open symbols). A benefit to radiation embrittlement resistance by a low copper content is clearly evident. Earlier determinations for low copper content A533-B materials from commercial scale demonstration tests are also given (small open symbols).

TABLE 1

MATERIALS AND HEAT TREATMENT

Material	Thickness cm	Thickness in.	Chemical Composition (Wt-%) Cu	P	C	Mn	S	Si	Ni	Cr	Mo	Al	Heat Treatment[a]
Series 3													
Plate 5	24.5	9.6	.02	.009	.20	1.24	.011	.23	.70	.05	.61	.027	1
Plate 6[b]	24.8	9.8	.04	.010	.24	1.28	.012	.24	.53	.09	.56	.023	1
Plate 7	24.8	9.8	.05	.007	.24	1.36	.011	.26	.56	.09	.58	.034	2
Weld 6 (SMA)	24.8	9.8	.03	.005	.097	1.01	.010	.39	.96	.01	.31	.001[c]	2
Series 2													
Plate 3	24.8	9.8	.09	.009	.20	1.29	.017	.22	.58	-d-	.57	.027	1
Plate 4	22.9	9.0	.09	.011	.21	1.38	.018	.28	.66	-d-	.52	.02	1
Weld 3 (S/A)	24.8	9.8	.07	.010	.15	1.15	.010	.25	.12	.04	.59	.004	2
Weld 4 (S/A)	22.9	9.0	.05	.004	.15	1.25	.010	.19	.09	.06	.62	<.001	2

[a]Heat Treatment: (1) Austenitized 871°C (1600°F) 4 hr, WQ; tempered 649-677°C (1200-1250°F) 4 hr, WQ; stress relief annealed 621°C (1150°F) 40 hr, furnace cooled to 316°C (600°F).

(2) Interstage stress relief annealed 593-621°C (1100-1150°F) 1/4 hr. minimum; postweld stress relief annealed 621°C (1150°F) 40 hr, furnace cooled to 316°C (600°F).

[b]Parent plate for Weld 6

[c]Soluble aluminum value

[d]Not determined

TABLE 2

Welding Parameters and Materials
(Series 3 Weld)

Weld Process	Shielded Metal Arc (SMA)
Electrode Type	E8018-C3
Electrode Diameter	4.75 mm (3/16 in.)
Voltage	25 V, dcrp
Current	210-260 amps
Travel Speed	26.7 cm/mm (10.5 ipm)
Preheat Temperature	149°C (300°F) minimum
Interpass Temperature	260°C (500°F) maximum

plan were 2 to 3×10^{19} and $5+\times 10^{19}$ n/cm^2 >1 MeV (ϕ^{fs}) for all materials. However, the irradiation plan was modified for the Series 3 materials in view of the performance of the Series 2 materials (high radiation resistance) and only "high fluence" experiments were performed. Experiment 1 (UCRR) with Plate 5 and HAZ 5 samples was irradiated to an average fluence of 5.3×10^{19} n/cm^1 >1 MeV; experiment 2 (UB) containing all materials except HAZ 5 reached fluences of 4.9 to 6.1×10^{19} n/cm^2 depending on experiment subsection.

Fluence determinations were based on measurements with iron neutron dosimeter wires included in each experiment specimen array. Irradiation period was of approximately 1500 hours duration for the UCRR experiment and of approximately 1900 hours for the UB experiment. Irradiation temperatures were monitored continuously by means of multiple thermocouples in each specimen group.

RESULTS AND DISCUSSION

Irradiation data developed for the six Series 3 materials are illustrated in Figs. 2-7 and are summarized in Table 3. Consistent with the low copper (and phosphorus) contents, all of the materials show excellent radiation resistance in terms of notch ductility retention. For example, Plates 5, 6, and 7 exhibited C_V 40.7 J (30 ft-lb) transition temperature increases on the order of only 36 to 42°C (65 to 75°F).

HAZ materials, although showing wide data scatter, were noted to have a transition temperature elevation comparable to the parent plate (e.g., HAZ 6) or less than the parent plate (e.g., HAZ 5). More importantly, postirradiation data for the HAZ fall consistently to the left of the postirradiation curve established for the parent plate in the transition region. (For Plate 5, the postirradiation curve for the LT orientation is assumed to follow the curve for the TL orientation in the transition regime based on preirradiation comparisons). In the upper shelf regime, HAZ comparisons are less clear. The data for HAZ 6 vs Plate 6 suggest a somewhat greater irradiation effect on the HAZ both in terms of upper shelf energy reduction and in terms of absolute values. A similar comparison for HAZ 5 vs Plate 5 was not possible for lack of plate LT orientation data. It is observed, however, that the postirradiation upper shelf of the HAZ is not reduced below that of the TL orientation of the plate in either case.

Referring to Fig. 7, the weld deposit depicted very high resistance to radiation, surpassing that of the Series 3 plates. The performance of this weld was of special interest because certain experimental data[1,4,5] previously

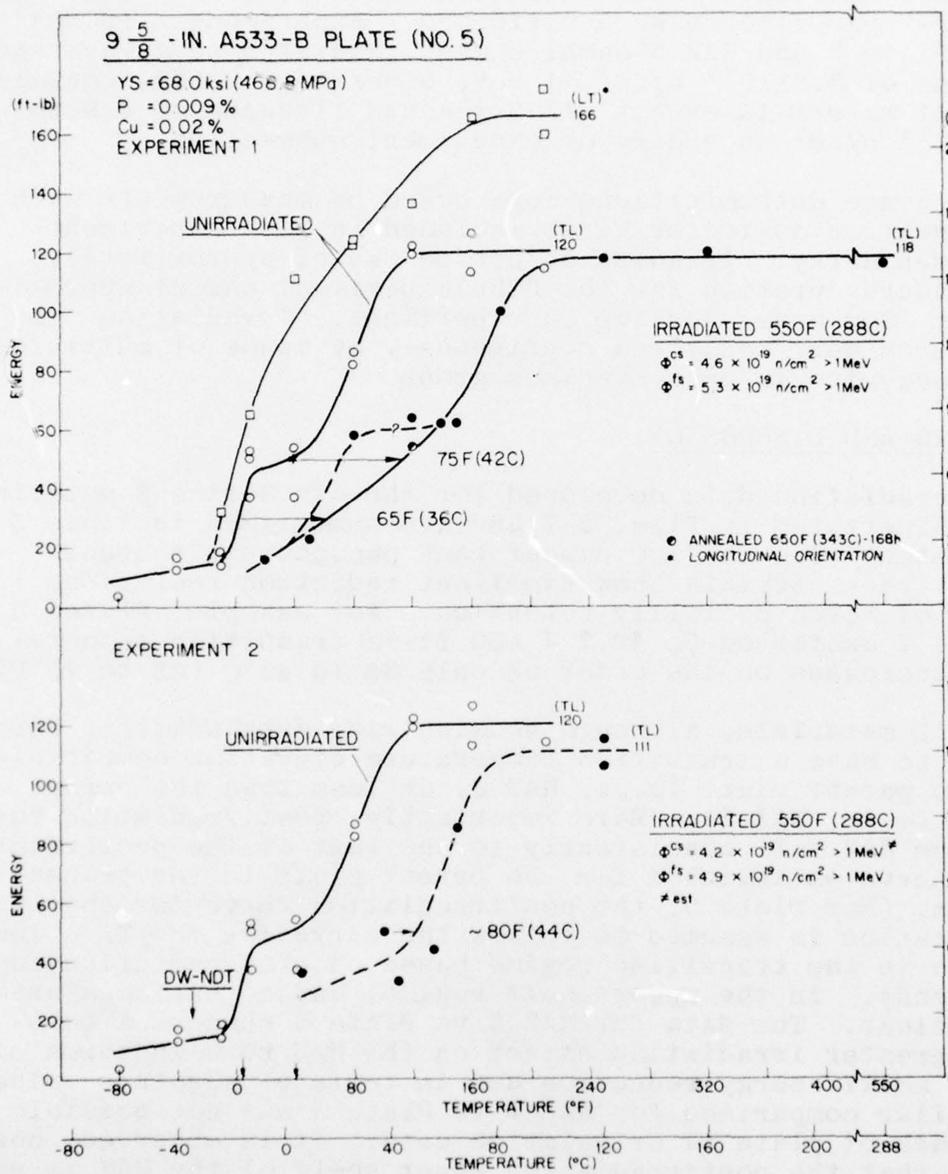

Fig. 2 — Notch ductility of Plate 5 (Series 3) before and after 288°C (550°F) irradiation to two fluence levels. In this figure and in Figs. 3-7, open and filled symbols refer to unirradiated and irradiated conditions, respectively.

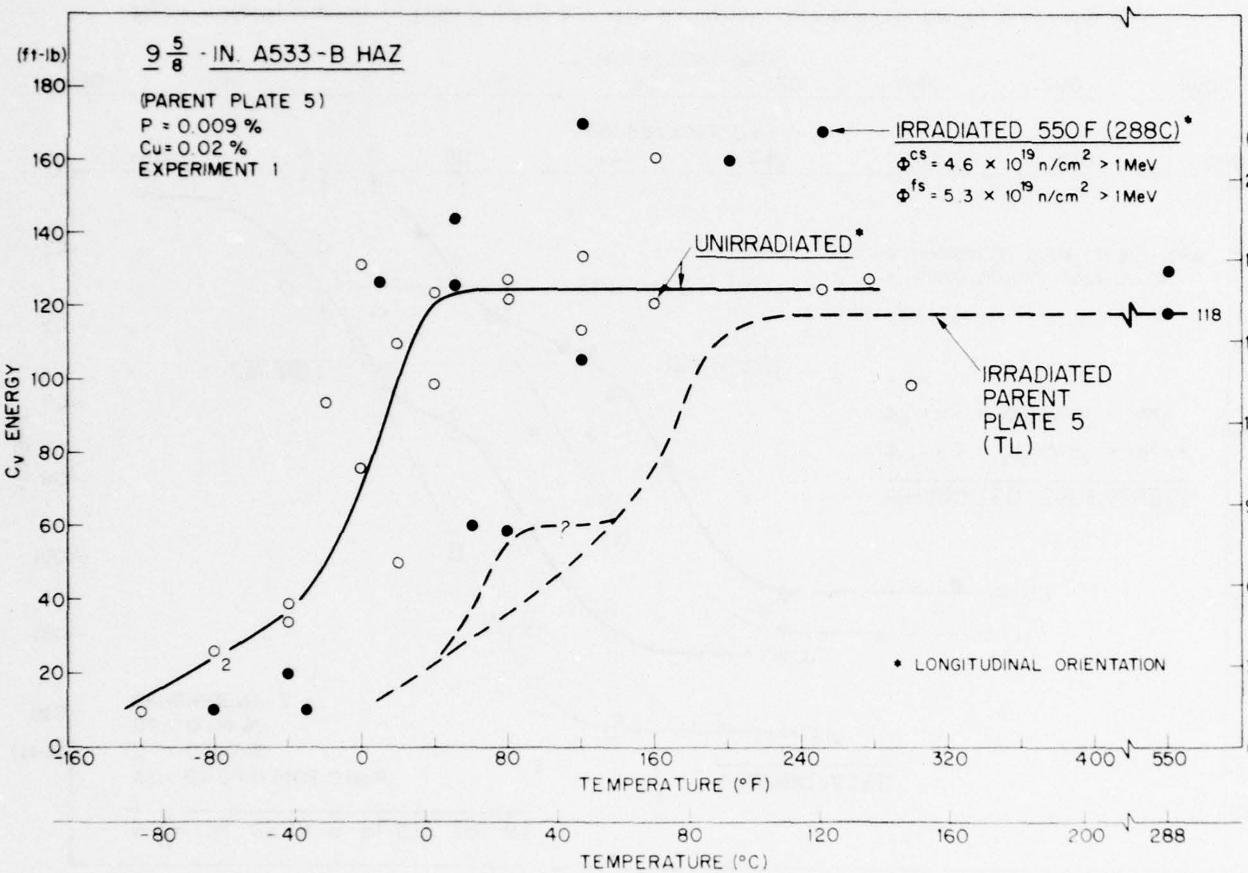

Fig. 3 — Notch ductility of HAZ 5 before and after irradiation. The notch ductility of the parent plate (TL orientation, Fig. 2) after irradiation is also indicated (dashed curve).

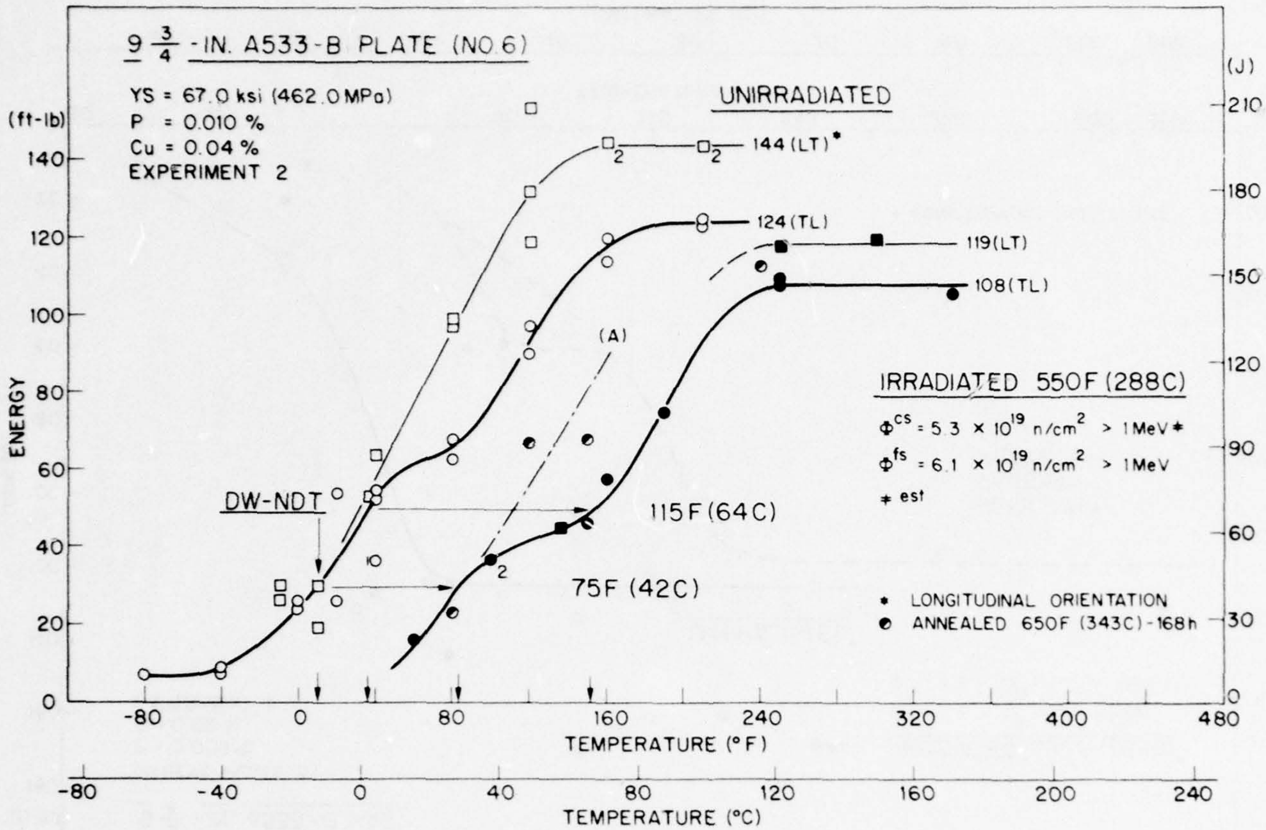

Fig. 4 — Notch ductility of Plate 6 before and after irradiation. Limited data for the postirradiation annealed condition (half filled symbols) are also shown.

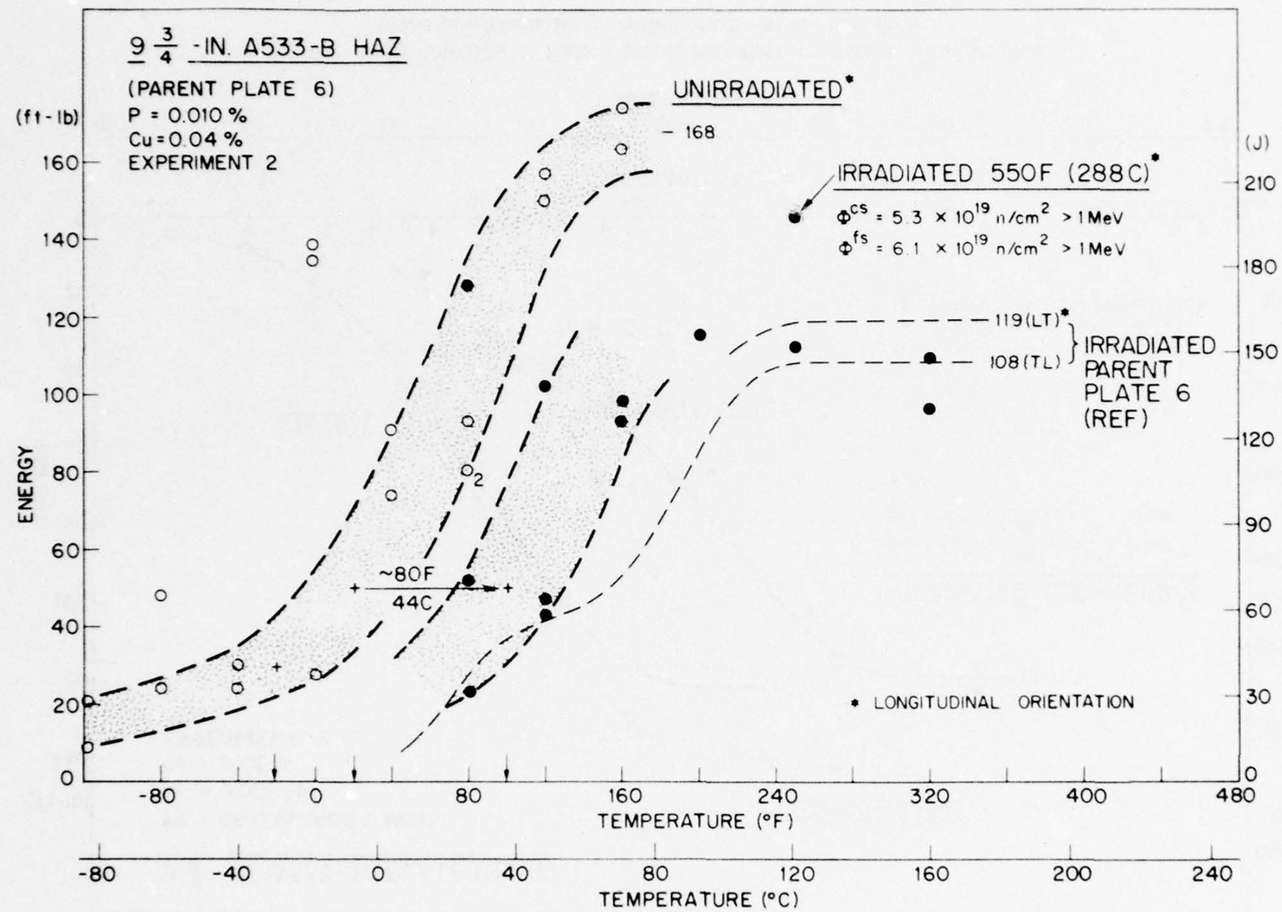

Fig. 5 — Notch ductility of HAZ 6 before and after irradiation. The notch ductility of the parent plate (LT and TL orientations, Fig. 4) after irradiation is also indicated.

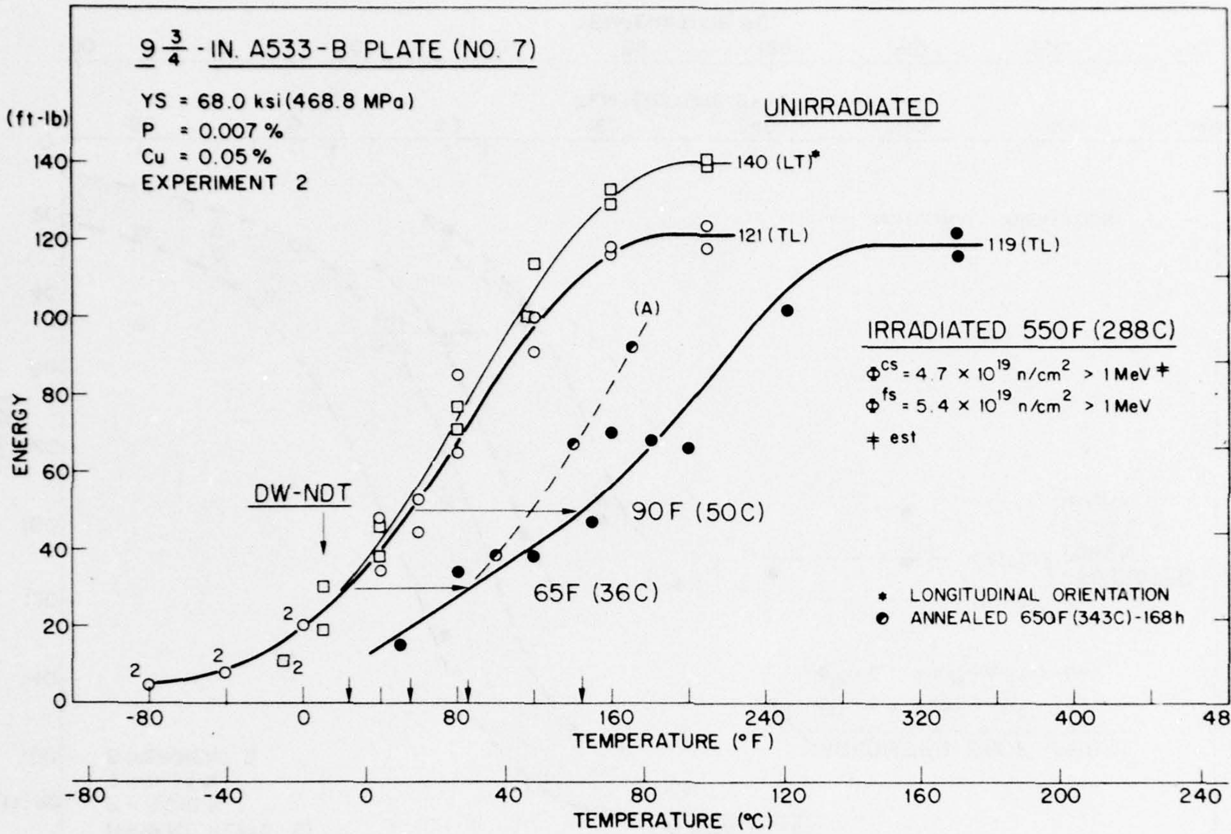

Fig. 6 — Notch ductility of Plate 7 before and after irradiation. Limited data for the postirradiation annealed condition are also shown.

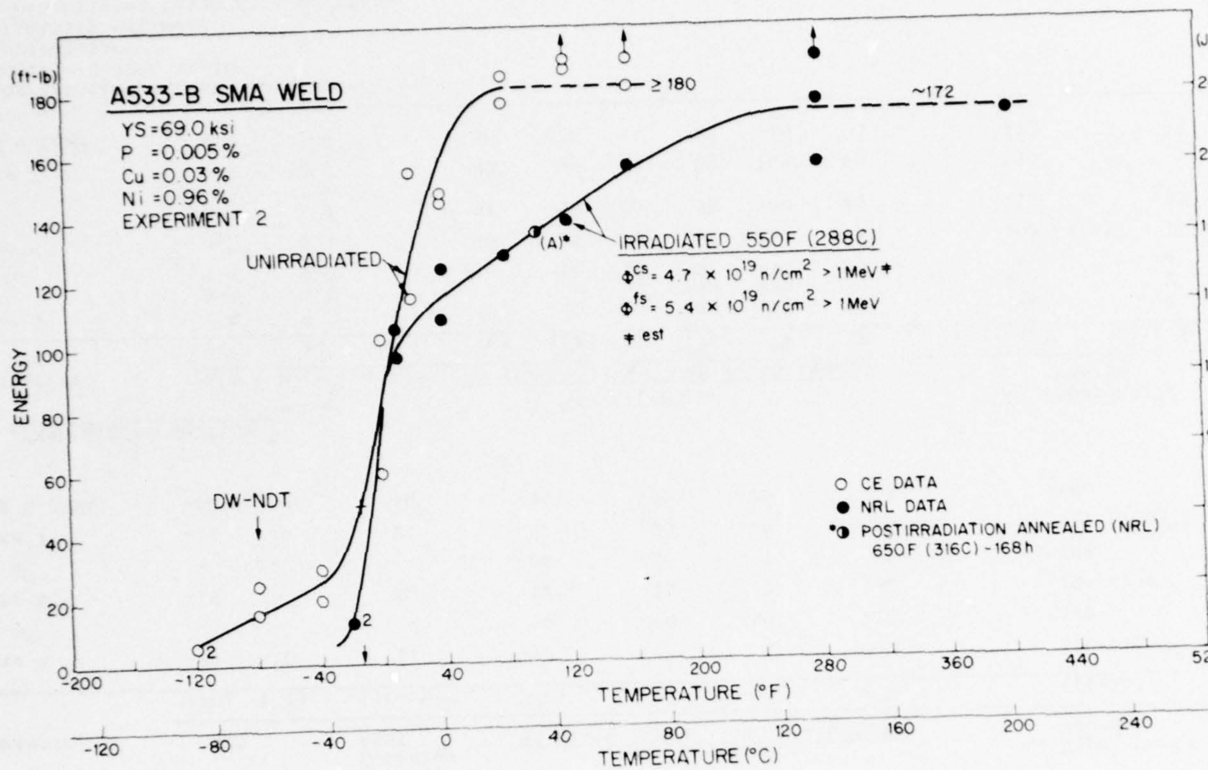

Fig. 7 — Notch ductility of Weld 6 (SMA) before and after irradiation. One datum for the postirradiation annealed condition is also shown.

TABLE 3

Notch Ductility Properties of Plates, Weld Deposit, and Weld Heat Affected Zones (HAZ) As-Fabricated and After 288°C (550°F) Irradiation

A. AS-FABRICATED[a]

Material	NDT		C_V Energy @NDT	C_V Transition				C_V Upper Shelf Energy
				30 ft-lb index		50 ft-lb index		
	(°C)	(°F)	(ft-lb)[b]	(°C)	(F°)	(°C)	(°F)	(ft-lb)
Plate 5	-34	-30	14	-18	0	4	40	120 (166)[c]
HAZ 5[c]	-	-	-	-51	-60	-29	-20	∿125
Plate 6	-18	0	30	-12	10	2	35	124 (144)[c]
HAZ 6[c]	-	-	-	-29	-20	- 7	20	∿168
Plate 7	-12	10	24	- 7	20	13	55	121 (140)[c]
Weld 6 (SMA)	-62	-80	16	-34	-30	-26	-15	≥180

B. IRRADIATED CONDITION [a]

Material	Fluence ($x10^{19}$ n/cm^2 >1 MeV)		C_v Transition						C_v Upper Shelf Energy	
			30 ft-lb index			50 ft-lb index				
	ϕ^{cs}	ϕ^{fs}	(°C)	(°F)	ΔF	(°C)	(°F)	ΔF	(ft-lb)	Δ(ft-lb)
Plate 5	4.6	5.3	18	65	65	46	115	75	118	2
	4.2[d]	4.9	e	e	e	∿49	∿120	80	111	9
HAZ 5	4.6	5.3	<10	<50	<110	<21	<70	<90	e	e
Plate 6	5.3[d]	6.1	29	85	75	66	150	115	108 (119)[c]	16 (25)[c]
HAZ 6	5.3[d]	6.1	21	∿70	∿90	38	100	80	≳115	≳53
Plate 7	4.7[d]	5.4	29	85	65	63	145	90	119	2
Weld 6 (SMA)	4.7[d]	5.4	-26	-15	15	-23	-10	5	∿172	≥8

[a]TL orientation except where noted.
[b]1 Joule = 0.7376 ft-lb
[c]LT orientation
[d]Preliminary estimate
[e]Not established (high data scatter)

had raised suspicions of a detrimental contribution of nickel content to radiation sensitivity in addition to that of copper. The materials in question consisted largely of high copper (> 0.20% Cu) weldments of A533-B steel. The NRL interpretation of the data was a reinforcement by nickel of the primary copper effect rather than an independent contribution of nickel to radiation resistance for nickel contents up to 1%.[1,4,5] An independent effect of nickel, on the other hand, was projected by other investigators.[6] Because of the broad use and importance of E8018-C3 electrodes (~1% Ni) for shielded metal arc welding of A533-B in nuclear construction, the existence and mode of a nickel contribution to radiation performance were critical uncertainties. The results of Fig. 7 clearly demonstrate that nickel does not contribute separately to radiation embrittlement sensitivity for amounts up to 1% Ni. NRL findings for a 0.6% Ni weld made by the submerged arc process provide separate supporting evidence. Thus, the original concern for the use of low copper content E8010-C3 electrodes for high fluence applications can be dismissed. The results, however, do <u>not</u> resolve suspicions of a nickel-content contribution to radiation behavior for the case of high copper welds since the possibility for a nickel-copper interaction first suggested by the NRL analysis remains.

In Fig. 8, the C_V 40.7J (30 ft-lb) transition temperature increases determined for the Series 3 materials are compared to previously reported data for the Series 1 and 2 materials. Significantly, comparable trends in radiation induced property changes are indicated for the extra low copper content materials vs the low copper content materials; that is, for the Series 3 materials and the demonstration test materials vs the Series 2 materials. The study accordingly has demonstrated that a further reduction in maximum allowable copper content from 0.10% Cu (ASTM specification) to 0.06% Cu (best steelmaking practice) will not result in particular benefit to radiation resistance, at least for plate and HAZ materials. For welds, the practical significance of 0.06% Cu max vs 0.10% Cu max was not actually investigated because of the similarity of copper contents (equally low). From Table 1, it is noted that weld copper contents were all in the range of 0.04 to 0.07% Cu. It is pointed out, however, that the welds with the lowest copper and phosphorus contents exhibited the highest radiation resistance of all the materials evaluated.

Limited results for postirradiation heat treatment (annealing) of Plates 6 and 7 are presented in Figs. 4 and 6. In both cases, 343°C (650°F)-168 hour annealing did not produce significant recovery in C_V 40.7J (30 ft-lb) transition temperature and produced only limited recovery in the

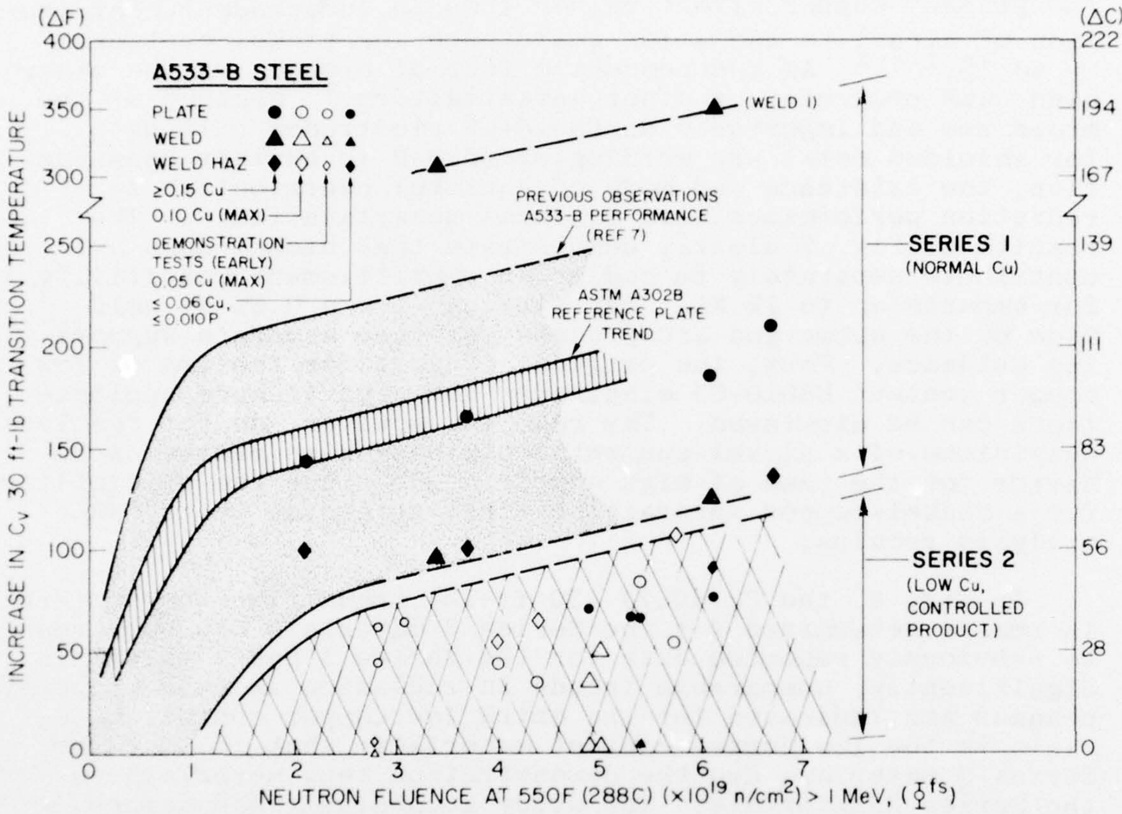

Fig. 8 — Summary of Charpy-V transition temperature observations for Series 3 materials (small filled symbols) superimposed on graph of Fig. 1. An entry (datum) for HAZ 5 was precluded by high data scatter. The results demonstrate comparable radiation resistance in materials with 0.06% Cu max and 0.10% Cu max contents respectively representing best steelmaking practice vs current improved practice.

C_V 67.8J (50 ft-lb) transition temperature. A high degree of recovery was not expected from earlier results. For materials showing high radiation resistance, embrittlement relief by annealing is not expected to be important for extending component lifetime; however, the current results do help extend the state-of-the-art on postirradiation annealing trends among steels.

CONCLUSIONS

Preliminary radiation assessments of the Series 3 materials (extra low copper content) from the NRC-CE-NRL Cooperative Program have results in the following primary observations and conclusions:

1. The specification of extra low copper content (0.06% Cu max, optimum steelmaking practice) as opposed to a low copper content (0.10% Cu max, improved practice only) does not provide a large increase in 288°C (550°F) radiation resistance for A533-B steel for fluences up to $\sim 5 \times 10^{19}$ n/cm^2 >1 MeV.

2. All plate, weld, and HAZ materials of Series 3 exhibited very low sensitivity to radiation induced change in C_V notch ductility in terms of transition temperature elevation and upper shelf energy degradation. Typically, C_V 30 ft-lb transition temperature elevations were less than 56°C (100°F) with fluences (ϕ^{CS}) of 4.6 to 5.3×10^{19} n/cm^2 >1 MeV.

3. The weld deposit showed the best radiation resistance of the Series 3 materials. The weld HAZ, in general, exhibited a ductile/brittle transition no higher than that of the parent plate. Somewhat poorer upper shelf retention by the HAZ is suggested by the data.

4. Nickel in amounts up to 1% does not contribute separately to radiation effects sensitivity in low copper content A533 welds.

5. Postirradiation annealing of extra low copper content A533 steel plates at 343°C (650°F)-168 hours is not highly effective toward radiation effects recovery.

A final report on this phase of the NRC-CE-NRL Cooperative Program is in preparation.* The report will include a summary of Series 1 and Series 2 material investigations as well.

---

*Joint NRL and CE authorship.

B. Influence of Phosphorus and Copper on Postirradiation Upper Shelf Performance of Steel

J. R. Hawthorne

BACKGROUND

The detrimental influence of phosphorus and copper impurities on the brittle/ductile transition behavior of low alloy steel under 288°C (550°F) irradiation is well established. The importance of these elements to upper shelf energy retention during irradiation and to upper shelf recovery behavior by heat treatment (annealing) on the other hand has not been explored in detail. The mechanisms for the phosphorus and copper contributions to radiation sensitivity are known to be different.[7,8] Accordingly, it is possible that one and not the other of these impurity elements exert an influence on upper shelf behavior with irradiation. It is equally possible that upper shelf degradation by radiation exposure is simply a function of relative "damage state" which is defined by material sensitivity level, regardless of the particular metallurgical factors involved, coupled with the fluence received.

PROGRESS

A recent investigation has explored the individual influences of copper and phosphorus on upper shelf behavior with 288°C (550°F) irradiation and with 343 and 371°C (650 and 700°F) postirradiation annealing. Four materials were employed and are identified in Table 4. Plate N27 served as a reference material. The materials were irradiated simultaneously in one reactor experiment to minimize exposure differences. Some small fluence (n/cm^2 >1 MeV) differences due to the reactor flux gradient were noted. The experiment include C_v specimens for typical notch ductility determinations and fatigue precracked Charpy-V specimens (PCC_v) for fracture toughness determinations (K_{Jd}) by the J-Integral method.

Table 5 summarizes findings for the C_v specimen assessments. Referring to the irradiated condition, greater embrittlement in terms of transition temperature increase with increasing copper and phosphorus content is indicated (expected trend). In contrast, absolute upper shelf energy decreases show no trend with copper level. In terms of percentage decrease, however, the performance of Plate N27 vs Plate 1T suggests a greater percentage decrease by irradiation with a higher copper content. Similarly, a greater effect by irradiation for increasing phosphorus content is

TABLE 4

A302-B and A533-B Materials Differing in Phosphorus and Copper Content

Material	Thickness (cm)	Chemical Composition-wt%							
		P	Cu	C	Mn	S	Si	Ni	Mo
A302-B Plate 40C	1.3	.021	.008	.23	1.30	.022	.21	-a-	.53
A533-B Plate N27	15.2	.008	.13	.17	1.21	.007	.20	.56	.50
A533-B Plate 1T	22.9	.012	.24	.22	1.30	.024	.28	.52	.40
A533-B Weld W1*	24.8	.020	.35	.09	1.45	.013	.68	.57	.39

-a- Not determined.
*Submerged arc weld.

TABLE 5

Irradiation and Postirradiation Annealing *Response of A302-B and A533-B* Materials Differing in %P and %Cu

I. 288°C (550°F) Irradiated Condition

Material	Material Code	Fluence (n/cm^2 >1 MeV) x10^{19}	Trans. Temp. Incr. C_v 30 ft-lb ΔT°C	C_v 30 ft-lb ΔT°F	C_v 50 ft-lb ΔT°C	C_v 50 ft-lb ΔT°F	Upper Shelf[a] ft-lb Irrad.	Upper Shelf ft-lb Decr.	Upper Shelf %
A302-B Plate (0.021P, 0.008 Cu)	40C	2.0	72	130	83	150	55	20	27
A533-B Plate (0.008P, 0.13 Cu)	N27	2.5	~72	~130	86	155	119	23	16
A533-B Plate (0.012P, 0.24 Cu)	IT	2.0	89	160	-	-	40	20	33
A533-B Weld (0.020P, 0.35 Cu)	W1	2.2	122	220	~122	~220	49	16	28

II. Postirradiation Annealed Condition

Material Code	343°C (650°F) - 168h Anneal: Trans. Temp. Recovery C_v 30 ft-lb ΔTR°C	C_v 30 ft-lb ΔTR°F	C_v 50 ft-lb ΔTR°C	C_v 50 ft-lb ΔTR°F	Upper Shelf Δft-lb	Upper Shelf %Rec	371°C (700°F) 168h Anneal: Trans. Temp. Recovery C_v 30 ft-lb ΔTR°C	C_v 30 ft-lb ΔTR°F	C_v 50 ft-lb ΔTR°C	C_v 50 ft-lb ΔTR°F	Upper Shelf Δft-lb	Upper Shelf %Rec
40C	~28	~50	33	60	12	60	-	-	-	-	14	70
N27	-	-	~50	~90	18	80	-	-	78	140	23	100
IT	~33	~60	-	-	8	40	-	-	-	-	20	100
W1	11	20	~17	~30	3	20	47	85	~39	~70	13	80

[a] J = 1.36 x ft-lb

suggested by the results for Plates N27 and 40C. Referring to results for the postirradiation annealed condition, two important determinations were possible. First, a decrease in upper shelf recovery with increasing copper content is demonstrated by the 343°C (650°F) data. Secondly, a difference of 28°C (50°F) in annealing temperature (i.e., 371 vs 343°C, 700 vs 650°F) can have a very marked effect on upper shelf response. For Plate 40C the data are tentative but suggest that phosphorus content is detrimental to recovery behavior as well.

Table 6 lists pre- and postirradiation fracture toughness (K_{Jd}) values for one plate and weld. All tests were conducted at 177°C (350°F) corresponding to the upper shelf regime. For Plate N27, upper shelf degradation with irradiation and recovery with annealing are clearly depicted. For weld W1, an inconsistency is noted relative to the C_v data trend, that is, the average K_{Jd} value for the unirradiated condition. This may be simply a manifestation of data scatter but could point up a potential problem in the use of the PCC_v test method, i.e., need for multiple specimen testing.

To summarize, results of this investigation signify an important role of copper and phosphorus impurities on postirradiation C_v upper shelf level, especially with postirradiation heat treatment. A follow-on study with a series of laboratory split melts with statistical impurity variations has been undertaken to provide a more definitive test of the impact of both copper and phosphorus on upper shelf trends.

TABLE 6

Fracture Toughness (K_{Jd}) of A533-B Plate and Weld from J-Integral Assessments of Precracked C_v Specimens

Material	Material Code	K_{Jd} [a] at 177°C (350°F)							
		Unirradiated		Irradiated		343°C (650°F) Annealed		371°C (700°F) Annealed	
Material		ksi√in.	MPa√m	ksi√in.	MPa√m	ksi√in.	MPa√m	ksi√in.	MPa√m
A533-B Plate (.008P, 0.13 Cu)	N27	207	227	151	166	192	211	191	210
		252	277	150	165	157	173	188	207
		273	300						
A533-B Weld (.020P, 0.35 Cu)	W1	149	164	143	157	162	178	162	178
		147	162	146	160	148	163		
						161[b]	177		

a $$K_{Jd} = \left[E\, J\, P_{max} \right]^{\frac{1}{2}}$$

b 93°C (200°F) Test

II. THERMAL SHOCK-RELATED INVESTIGATIONS

A. Characterization of Warm Prestress Phenomenon

F. J. Loss, R. A. Gray, Jr. and J. R. Hawthorne

BACKGROUND

One of the postulated events for a nuclear pressure vessel is a sudden loss of coolant accident (LOCA) followed by operation of the emergency core cooling system (ECCS). Introduction of the relatively cold ECCS water subjects the vessel wall to high thermal stresses, i.e., thermal shock, that can lead to extension of a preexisting flaw. It has been assumed that crack extension will initiate when the applied K_I level at the flaw tip achieves the critical K_{Ic} level. However, crack extension may not actually take place if K_I is decreasing with time when the K_{Ic} level is attained. This phenomenon is known as "warm prestress" (WPS).

Since K_{Ic} is a function of temperature, its value can exceed the peak applied K_I level early in time when the vessel wall is hot. In this event crack extension will not take place as the peak K_I is applied. Later, both the K_I level and the wall temperature, and therefore K_{Ic}, decrease at different rates; this behavior can result in an equivalence between K_I and K_{Ic}. At this time, however, the prior WPS at the crack tip is expected to preclude crack extension.

An experimental program is underway to characterize the WPS phenomenon and to define its potential benefits in terms of inhibiting crack extension in a nuclear vessel. The experimental program employs notched, 3-point bend specimens of A533-B Class 1 steel. Specimens are subjected to a K_I vs temperature path that simulates the conditions during a LOCA. The experimental procedure has been described in Ref. 7. The first phase of the WPS experiments has been completed and the results are summarized here.

EXPERIMENTAL RESULTS

Results from 38mm and 76mm (1.5 and 3.0 in.) thick bend specimens are presented in Figs. 9 and 10, respectively. In both figures, specimens were loaded to a predetermined K_I level at room temperature (i.e., warm prestressed) and then simultaneously unloaded and cooled to a given temperature. This was followed by an isothermal loading to failure. The figures illustrate the behavior of two specimen loading patterns. The filled symbols denote a partial unloading (e.g., 30-60%) over the increment, ΔT, between the temperature of WPS (T_{wps}) and the temperature of isothermal loading to failure (T_F). The open symbols denote complete unloading

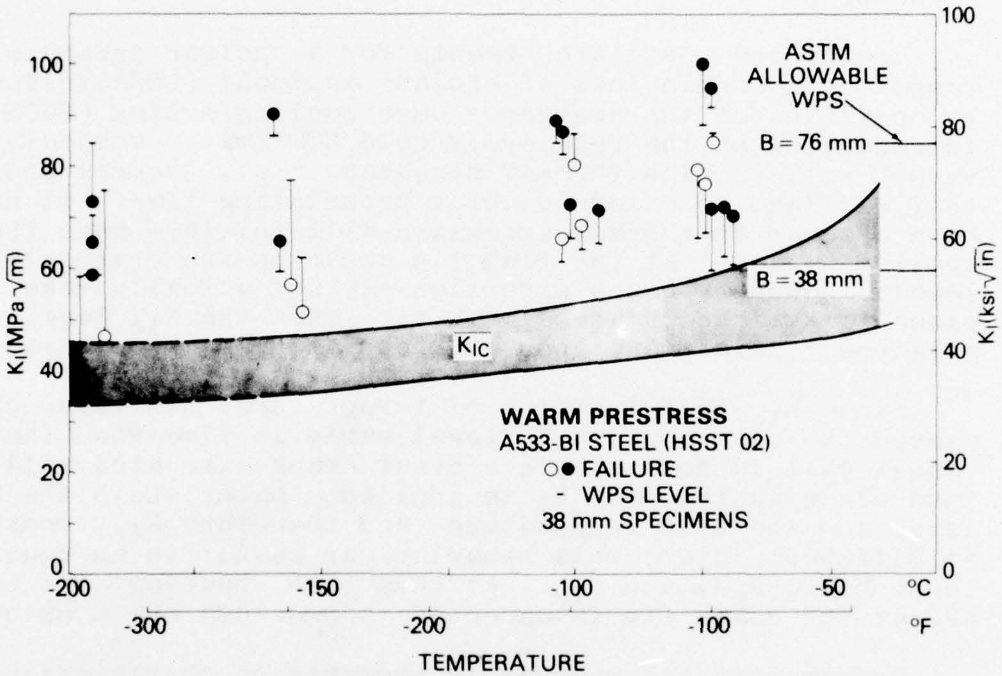

Fig. 9 — Warm prestress trends for 38 mm (1.5 in.) thickness specimens. Specimens received a warm prestress loading at room temperature to the levels indicated. Filled symbols denote partial unloading while open symbols denote the failure path "load, unload, cool, fracture" (LUCF).

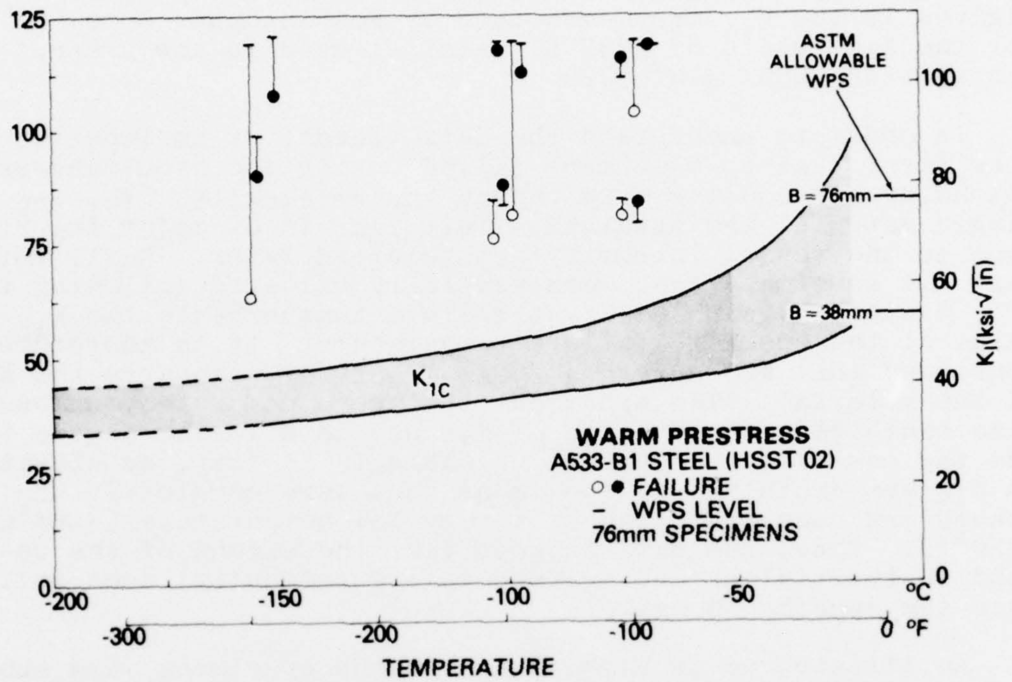

Fig. 10 — Warm prestress trends for 76 mm (3 in.) thickness specimens. Specimens received a warm prestress loading at room temperature to the levels indicated. Symbols are defined in Fig. 9.

at T_{wps}, cooling to T_F and failure by subsequent isothermal loading (LUCF). It must be emphasized that only the partial unloading path is representative of LOCA conditions in that complete unloading will not occur during the accident. The LUCF path, however, provided a means to characterize the significance of the degree of unloading. Also shown in the figures is the K_{Ic} trend measured by Westinghouse Corp.[9,10] for the same plate of A533-B1 material used in the present investigation (HSST plate 02).

In order to understand the data trends, it is important to note first that no specimens failed during the simultaneous unloading and cooling even though the critical K_{Ic} for the virgin material was attained. This fact is of major importance to the vessel integrity as explained later. Next, note that all specimens that were partially unloaded following the WPS, exhibit a value of K_I at failure that exceeds the K_{Ic} value at the specific failure temperature. It is therefore concluded that WPS during a LOCA effectively elevates the K_{Ic} of the material. The specimens that were completely unloaded also exhibited an elevation of K_{Ic} but to a lesser degree than was the case for the partial unloading. In fact, no elevation in K_{Ic} was exhibited by specimens that were completely unloaded and then fractured at a very low temperature (-196°C, -320°F). Thus, the data suggest that the extent of the unloading (partial unloading vs complete unloading) does influence the specimen behavior.

As illustrated in Figs. 9 and 10 the specimens were subjected to different levels of WPS. The lower level in each case corresponds to the ASTM E399 allowable for the specific thickness. With the 38mm specimens (Fig. 9) the higher WPS level corresponds to that which is permitted for a specimen of 76mm or greater thickness. For the 76mm specimens the higher WPS level corresponds to the allowable value for a 152mm (6 in.) or greater thickness specimen. No differences are apparent between the trends for the 38mm specimens prestressed to 80 MPa$\sqrt{m}$ (the ASTM allowable for a 76mm specimen) in Fig. 9 and those in Fig. 10 for the 76mm specimen prestressed to the same level. Also, a similar fracture surface appearance was observed for both specimen thicknesses. This correspondence suggests that the larger plastic zone size resulting from the "overload", to 80 MPa$\sqrt{m}$, of the 38mm specimens is not a deterrent factor in assessing the effects of WPS. On this basis, it is concluded that the geometrically similar overload of the 76mm specimens, to approximately 120 MPa$\sqrt{m}$, (Fig. 10) would also represent the behavior of 152mm thick specimens, had they been available for test. This conclusion is significant in that it permits a more general interpretation of the benefits of WPS to the higher K levels that may be experienced by a vessel during a LOCA.

ANALYSIS OF DATA

The magnitude of the K_{Ic} elevation by WPS may be observed from Figs. 9 and 10. It is not possible to assign a quantitative value to this elevation in terms of, say, K_F/K_{Ic} since the failure level, K_F, depends upon (a) WPS level (K_{wps}) (b) failure temperature, and (c) degree of unloading. However, it should be noted that for a given failure temperature and unloading path, K_{Ic} is elevated in proportion to the magnitude of K_{wps}. Thus, it appears that a high value of K_{Ic} could be obtained at a very low temperature simply through the application of a high level of K_{wps}.

The preceding is a simplistic analysis of the WPS phenomenon. Therefore, it is of benefit to consider the interaction of the three major independent parameters listed above and depicted in Fig. 11. From this figure it can be concluded that the maximum benefit of WPS, in terms of the highest K_F/K_{wps} ratio, is obtained for the case of partial unloading for which ΔT is small and the K_{wps} is low. Fortunately, during a LOCA, two of the above three conditions are met. First, the metal at the crack tip is always partially unloaded and this unloading is not expected to exceed the 30-60% to which the specimens were subjected. Second, the ΔT is expected to be small between the temperature of peak applied K_I during a LOCA and the temperature at which K_I attains the K_{Ic} level. That is to say, a ΔT of 100°C, corresponding to a T_F of -73°C in Fig. 11, may represent the largest value that could occur during a LOCA. Consequently, the partial unloading data at -73°C would be most applicable to a LOCA. From this, it can be concluded that for K_{wps} less than 120 MPa$\sqrt{m}$ (109 ksi$\sqrt{in.}$), the WPS phenomenon will (a) provide an effective elevation of K_{Ic} and (b) assure that the failure level will equal or exceed the level of WPS.

An alternate way to interpret the interaction of WPS level, failure temperature, and degree of unloading is presented in Fig. 12. This figure clearly illustrates that the elevation in K_{Ic}, as reflected by K_F, increases with WPS level. The magnitude of the K_{Ic} elevation can be observed by comparing K_F with the mean $\bar{K}_{Ic}$ values for the appropriate failure temperature. For example, a K_{Ic} elevation in excess of 200% is exhibited by the extreme of the partial unloading data at -73°C; whereas essentially no elevation in K_{Ic} is exhibited by the LUCF data at -196°C.

An extrapolation of the trend illustrated in Fig. 12 suggests that even higher elevations in K_{Ic} could be obtained with the higher imposed values of K_{wps}. Unfortunately, the data deviate from the one-to-one relationship between K_F and K_{wps} as K_{wps} is increased. The reason for this deviation is

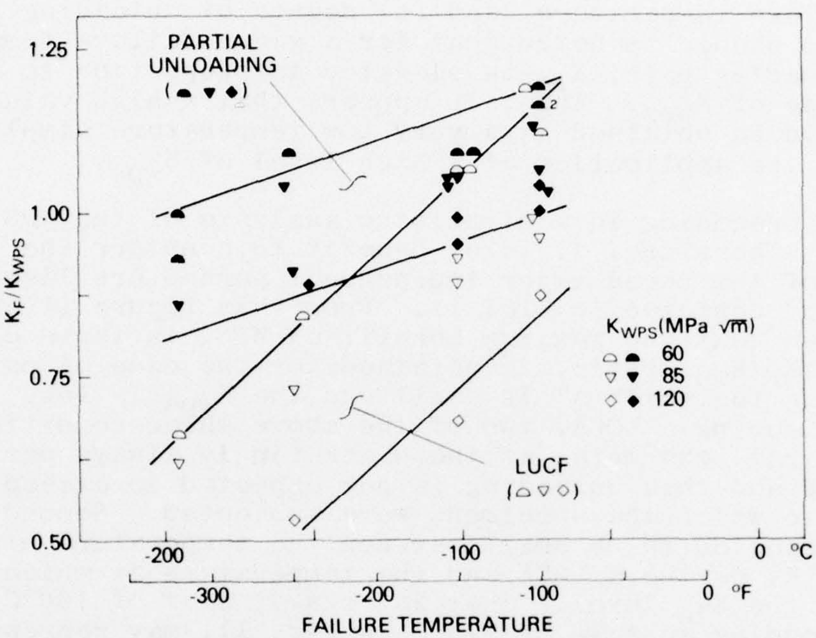

Fig. 11 — Relationship between the K_I at failure (K_F) and the level of warm prestress (K_{wps}) at room temperature as a function of K_{wps} level, unloading path, and failure temperature (T_F). The LUCF unloading path refers to load, unload, cool, fracture.

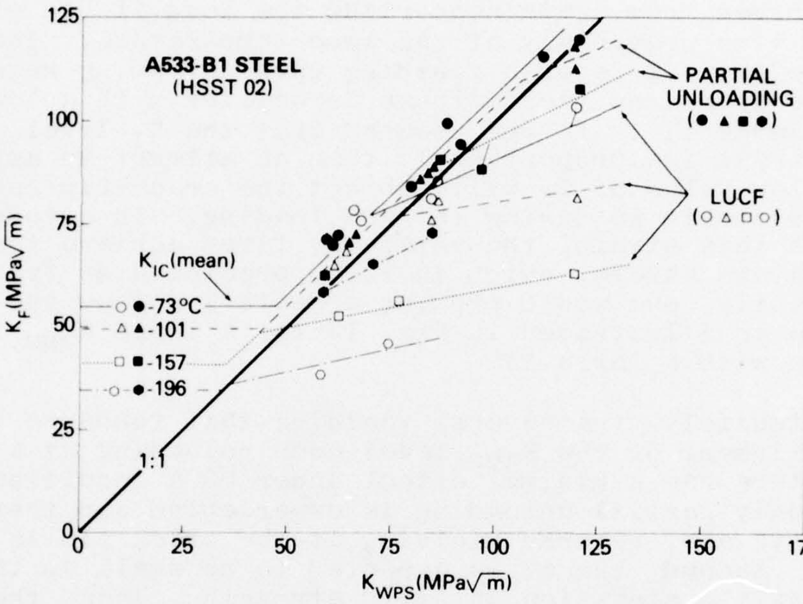

Fig. 12 — Comparison of the K_I at failure (K_F) with the level of warm prestress (K_{wps}) at room temperature. Warm prestress produces an artificial elevation in K_{Ic}. However, the relationship between K_F and K_{wps} depends upon the loading path, K_{wps} level, and the failure temperature. The latter is denoted on each data trend line.

believed to be related to the interaction of (a) the compressive residual stresses that can cause reverse yielding upon unloading of the crack tip, and (b) the temperature elevation of the yield stress that results when a large ΔT is employed. When ΔT is zero there can be no yield stress elevation. In this case, one would expect K_F to equal or slightly exceed K_{wps} in that no mechanism exists to prevent the specimen from again supporting the load it had withstood a short time previously at the same temperature. The detrimental effect of reverse yielding upon unloading results from the increased yield stress associated with a low value of T_F (large ΔT). If one assumes that the K_I level and local strain are proportional, then an attempt to apply K_{wps} at the low value of T_F will subject the crack-tip region to the same strain as during the WPS loading. In attempting to reach this strain, the metal may first achieve the critical cleavage stress, which in turn, precipitates fracture. Consequently, one would predict a deviation from the one-to-one line as illustrated in Fig. 12 for a large K_{wps} in combination with a large ΔT.

Fortunately, the reverse yielding that tends to prevent the attainment of the K_{wps} level upon reloading at a lower temperature has a minimal effect under LOCA conditions. First, only partial unloading is experienced and therefore little, if any, reverse yielding at the crack tip is expected. Second, the ΔT is expected to be small so there can be little elevation in yield strength. Thus, the critical cleavage stress can be achieved only at a K_F level that is not significantly below the original value of K_{wps}.

The above model appears to offer a satisfactory explanation for the observed trends in Fig. 12. Specifically, the large elevations in yield strength in the experimental program that resulted from the relatively large ΔT values (95 to 220°C) are not expected to occur during a LOCA. Consequently, that portion of the data in Fig. 12 most directly applicable to the LOCA conditions (i.e., partial unloading and failure temperature of -73°C) supports the conclusion that WPS can be effective in preventing crack extension during a LOCA. The structural implications of WPS to a LOCA are considered next.

STRUCTURAL INTERPRETATION OF WPS DURING A LOCA

A theoretical analysis of the potential for crack extension during a LOCA has been performed by Cheverton[11] for a typical pressurized water reactor vessel. His results are interpreted here to characterize the maximum depth of crack extension when considering the influence of WPS. The time-dependent stress intensities computed from Cheverton's

analysis for a long, axial crack are presented in Figs. 13-15. The following assumptions were made in modeling the vessel:

- Wall thickness = 216 mm (8.5 in.).
- Inner wall fluence = 4×10^{19} n/cm^2 >1 MeV (corresponding to a 40-year irradiation period).
- High impurity copper level (> 0.25%).
- Preirradiation K_{Ic} vs temperature as defined by Westinghouse Corporation[9,10] for A533-B1 steel.
- Vessel not pressurized.

During a LOCA, the magnitude of possible crack extension cannot be easily computed. This fact has raised the possibility of complete crack penetration of the wall. Fortunately, the factors of decreasing fluence and increasing temperature toward the outside wall surface provide the mechanism for the arrest of a running crack that may initiate in the material of relatively low toughness near the inner wall surface. Arrest is assumed to occur when the K_{IR}* value exceeds the K_I value at the crack tip. Furthermore, the degradation in K_{IR} caused by neutron bombardment through the wall has been characterized in the subject analysis according to the procedures of Regulatory Guide 1.99.[12] The latter defines the K_{IR} vs temperature trend for irradiated material by a simple temperature translation of the preirradiation trend, based on the fluence level and residual impurity content of the steel. The K_{Ic} vs temperature trend for the irradiated material has been similarly projected. The validity of the latter assumption, however, is subject to additional verification.

Figure 13 illustrates the K_I level for a long axial flaw 7.5 minutes after the LOCA initiation. From the first intersection of K_I and K_{Ic}, it is concluded that an axial crack having a depth-to-wall thickness ratio (a/W) of 0.03 will initiate at this time. The flaw will propagate to a relative depth of a/W = 0.36 before it is assumed to arrest. It should be noted that different size flaws can initiate at different times. In other words, Fig. 13 represents crack initiation conditions only at 7.5 minutes.

A crossplot of the intersections of K_I with K_{Ic} and K_{IR} at various times is shown in Fig. 14. The dashed line illustrates the progressive initiation-arrest-reinitiation behavior of a shallow crack. This description suggests

*The K_{IR} vs temperature behavior for unirradiated material is defined in Section III of the ASME Boiler and Pressure Vessel Code. The mechanics of crack arrest is a topic of current research and presently one cannot guarantee that crack arrest will occur exactly when $K_{Ic} = K_{IR}$.

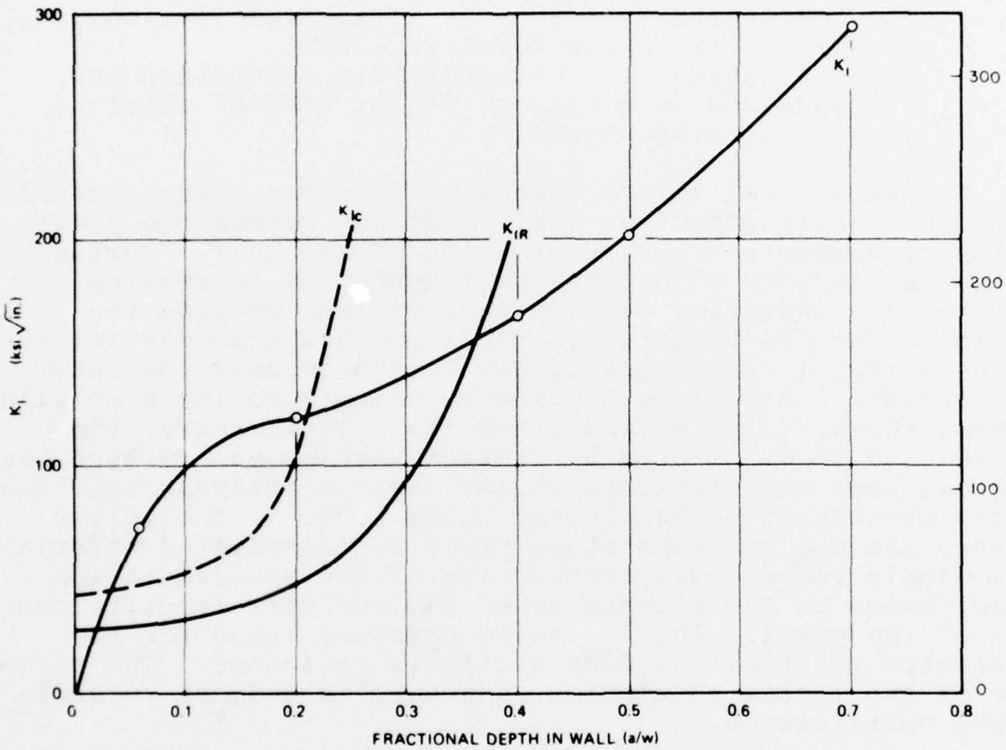

Fig. 13 — The K_I level for long, axial flaws of different depths in the reference vessel at a time of 7.5 minutes after the LOCA initiation. Critical crack depths for initiation (K_{Ic}) and arrest (K_{IR}) are also illustrated. (Ref. 11)

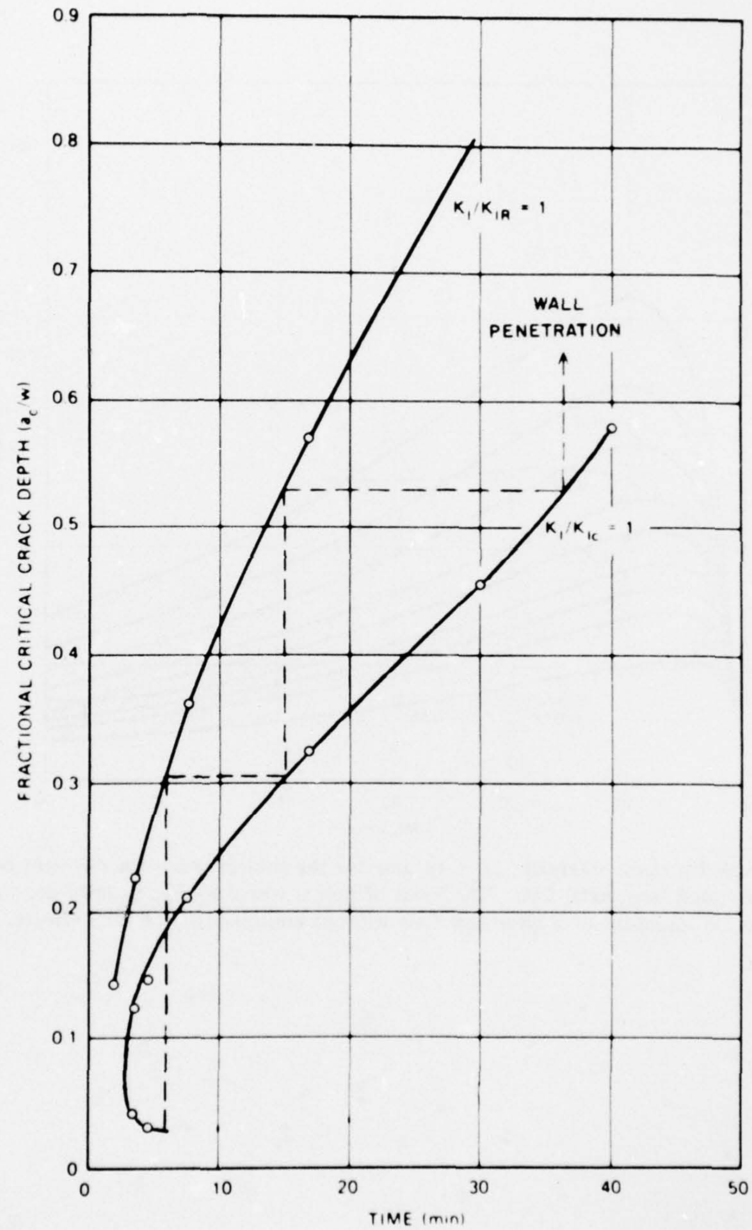

Fig. 14 — Critical crack depths for initiation and arrest with a long, axial flaw in the subject vessel. The dashed line denotes the progressive initiation-arrest-reinitiation behavior that could lead to deep penetration of the wall without consideration of the WPS phenomenon. (Ref. 11)

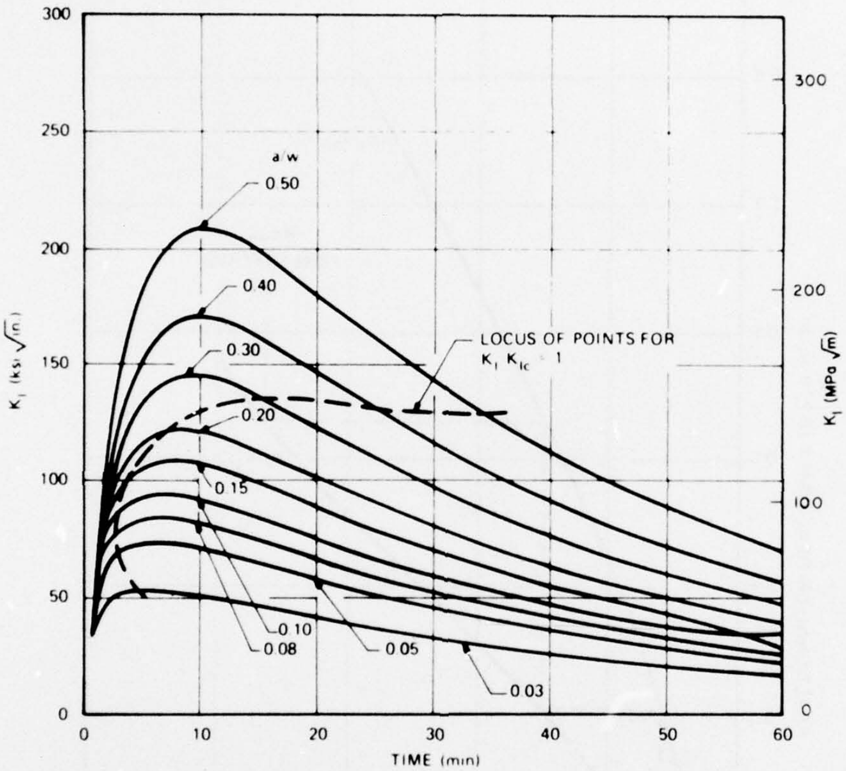

Fig. 15 — Crack tip stress intensity, (K_I), vs time for the subject vessel for different depths, a/w, of a postulated long, axial flaw. The locus of points where K_I/K_{Ic} is unity denotes the predicted time of initiation of a given size flaw without consideration of WPS effects. (Ref. 11)

that the crack could deeply penetrate the wall. However, Cheverton[11] has pointed out that the assumptions of his model are conservative and that complete wall penetration may not actually take place. Specifically the K_{Ic} calculations were based on linear elastic behavior. For large crack penetrations ($a/W>0.5$) the remaining ligament is subjected to plastic deformation and the assumption of linear elastic behavior is not valid. The presence of plasticity will result in K_I levels less than those computed elastically and therefore will decrease the propensity to penetrate the wall.

Figure 15 depicts the behavior of K_I with time for a family of long, axial flaws. It is important to note the relationship between these curves and the locus of points for which K_I/K_{Ic} is unity. With flaws of relative depth greater than 0.2, it is clear that the intersection of K_I and K_{Ic} occurs with decreasing K_I. This points out that all cracks greater than a relative depth of 0.2 have been warm prestressed. On the basis of the NRL investigations, it is therefore expected that cracks greater than this depth will not initiate in the subject vessel. Given the above, it is possible, nevertheless, to predict crack extension to relative depths greater than 0.2. Consider a flaw of relative depth of 0.1 in the framework of Fig. 14. Since this flaw is not subject to WPS, it will begin to extend at a time of 3 minutes and penetrate to a relative depth of 0.2. Because only cracks of relative depth greater than 0.2 are subject to WPS, the crack will reinitiate at a time of 7 minutes and extend to a relative depth of 0.34. Further extension is not likely because of WPS during the time periods up to 18 minutes when the next initiation would be predicted in the absence of WPS.

The preceding description illustrates that while crack initiation from shallow cracks cannot be prevented by WPS, the magnitude of the crack extension can be limited by this phenomenon so as to preclude complete penetration of the wall. The benefit of WPS is such that a potentially severe accident, that of complete wall penetration, is reduced to one of lesser severity in which the vessel integrity is maintained.

SUMMARY AND CONCLUSIONS

The present research investigations have considered the phenomenon of warm prestress and its potential benefit for the minimization of crack extension during a LOCA. It is concluded that the mechanisms associated with WPS act to elevate the critical fracture toughness, K_{Ic}, of the material at the crack tip. During a LOCA, an elevation of K_{Ic} results

when the peak value of WPS (K_{wps}) is applied at a sufficiently high temperature so that the K_{Ic} of the material exceeds K_{wps}. After this peak loading to K_{wps} the K_I level in the vessel decreases and achieves the critical K_{Ic} value at lower temperature (because of the temperature dependence of K_{Ic}). This study has demonstrated that failure never occurs during unloading. This observation is of major significance to the integrity of a prototype vessel. From this behavior it is concluded that crack initiation will not take place in a vessel once the crack tip has been subjected to WPS. This conclusion is valid irrespective of either the degree to which K_I at the crack tip falls below K_{Ic} or the nature of the unloading path. In other words, crack extension after WPS can take place only with increasing K_I; since K_I does not increase after the peak K_{wps}, no mechanism exists upon which to postulate crack extension.

In terms of margin of safety against fracture, this study has shown that the elevation in K_{Ic} caused by WPS is not uniform and depends upon (a) the WPS level, (b) the ΔT between the failure temperature and the temperature of WPS, and (c) the degree of unloading. Specifically, the beneficial elevation of K_{Ic} appears to be greatest when both the ΔT and the degree of unloading are small. Fortunately, both of these conditions are met during a LOCA, and an elevation of K_{Ic} should be assured by the WPS phenomenon. In particular, it is concluded that WPS levels of 120 MPa$\sqrt{m}$ or less can result in an elevation of K_{Ic} for the vessel material to at least the WPS level during a LOCA transient, assuming of course, that the material is metallurgically capable of exhibiting this level of toughness.

In these experiments, a relatively large ΔT was necessitated in order to unambiguously demonstrate the elevation of K_{Ic} by WPS. During the LOCA however, the ΔT can be much smaller than the values investigated. It is felt that a small ΔT will result in even greater benefit of WPS than demonstrated by this study. Nevertheless, experimental investigations are continuing at NRL to characterize the WPS phenomenon in the case of a small ΔT.

It has been suggested that the use of uniaxially-stressed bend specimens in the present investigation does not permit simulation of the biaxial loading that occurs in the vessel during a LOCA. However, the influence of biaxial loading in the linear elastic regime is not considered to be significant and should not alter the conclusions of the present investigation. A partial verification of this hypothesis results from a comparison of the data from the uniform specimens vs specimens having face grooves. Although not exactly similar, face grooves tend to increase the crack-tip constraint.

However, the data have shown that no trend was effected by the face-grooving. Nevertheless, the significance of biaxial loading during WPS has not been conclusively demonstrated. It appears that further analysis is required to resolve this area.

An interpretation of the structural significance of WPS has been made for a typical reactor pressure vessel containing a long-axial flaw and whose wall has been severely embrittled. Based upon an interpretation of K_I trends for this vessel computed by ORNL,[11] it is concluded that WPS by itself cannot prevent the extension of shallow cracks. However, for the reference vessel containing a long-axial flaw, it is concluded that: (a) a shallow crack (a/W <0.2) can initiate and extend to a relative depth of 0.34, and (b) a crack of initial relative depth greater than 0.2 is prevented from extending any amount by the WPS phenomenon. While the preceding interpretation of WPS to a reactor pressure vessel was meant to consider the worst case, a general conclusion regarding the significance of WPS to the mitigation of crack extension during a LOCA requires a parametric analysis to be made that considers different initial flaw geometries as well as differences in K_{I_c} trends, fluence and material sensitivity to irradiation.

Also, it was observed that an elastic analysis of crack extension during a LOCA has predicted deep penetration of the wall without consideration of WPS. Due to the conservatism in the elastic analysis, complete penetration of the wall may not actually occur. Nevertheless, the crack extension computed more exactly by means of a refined elastic-plastic model cannot be easily verified by full-scale experiments. Thus, the WPS phenomenon may eliminate the need for further elastic plastic computations and, more importantly, may provide the key element upon which to predicate the integrity of the vessel during a LOCA.

Finally, the following recommendations are considered necessary (a) to verify assumptions of the present analysis, and (b) to generalize the benefits of warm prestress to other geometries and material properties.

- Perform a sensitivity analysis to characterize the interaction of the significant parameters
- Validate the assumption that crack arrest is defined by the condition, $K_I = K_{IR}$.
- Provide a technical basis to disregard the effects of biaxial loading that occur during a LOCA that were not specifically considered in the experiments

- Verify the assumptions: (a) the shape of the irradiated K_{Ic} and K_{IR} vs temperature curves is unaltered by irradiation, and (b) the temperature elevation of the K_{Ic} curve due to irradiation is equal to or less than the elevation of the K_{IR} curve as defined by Regulatory Guide 1.99.

B. Plastic Net Ligament Studies

R. A. Gray, Jr., G. Sica and F. J. Loss

BACKGROUND

The preceding section considered the propensity for crack extension in the wall of a nuclear pressure vessel during a loss of coolant accident (LOCA). It was demonstrated that the phenomenon of warm prestress (WPS) can prevent crack extension beyond relative wall depths (a/w) of one-third. In order to demonstrate a still greater margin of safety against complete wall penetration, a second investigation was conducted wherein no credit was taken for the inhibition of crack extension by WPS. In this case, it is assumed that a crack can be driven almost completely through the wall by the thermal stresses associated with the LOCA. The purpose of the subject investigation is to demonstrate that further extension of the arrested crack will not be caused by the thermally-induced bending of the wall.

It should be recalled from the preceding investigation of WPS that the factors of decreasing neutron fluence and increasing temperature toward the outside wall surface produce a steep gradient in toughness that provides a mechanism for the arrest of a running crack. On this basis, one can consider as the worst case a long, axial flaw that has penetrated deeply through the vessel wall (e.g., a/w = 0.8) and has been arrested. Under these circumstances the remaining ligament is subject to a rotation, Θ, due to the thermal stress distribution in the wall. This rotation also results in a "cusp" of the vessel wall as illustrated in Fig. 16. The bending at the crack tip can cause a plastic hinging of the remaining ligament provided, of course, the material has sufficient toughness to preclude brittle fracture under this imposed loading. Fortunately, the rotation of this "plastic net ligament" is self-limiting by the thermal stresses. Using the temperature distribution in the wall of a typical vessel during a LOCA,[11] Merkle [13] showed that the bend angle would be no larger than 2° in the case of a crack having a relative depth of 0.8 in a wall of 216mm (8.5 in.) thickness.

If one assumes the arrested crack is subjected to a bend angle of 2°, some crack extension at the crack tip is expected.

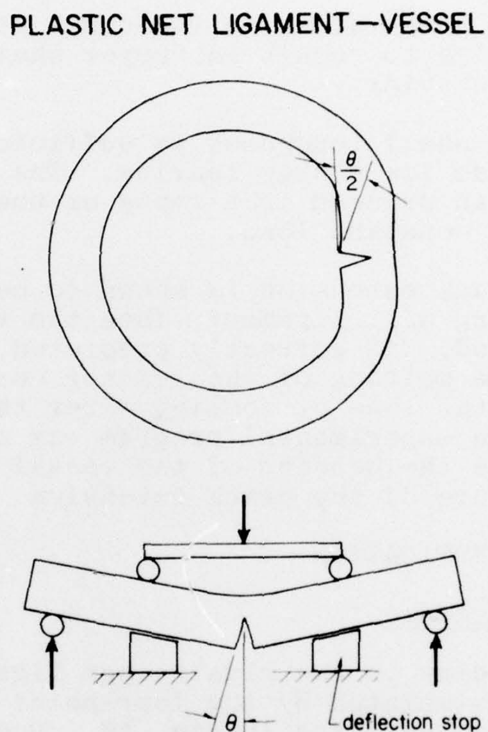

Fig. 16 — Illustration of the bending of the vessel wall that results from the thermal stresses imposed during a LOCA. The deep, axial flaw in the vessel wall is simulated by the bending of a cracked beam.

This extension will be stable (occurring with rising load) rather than unstable (brittle) under the following conditions:

- The toughness of the material at the tip of a deep crack has not been severely degraded by the neutron bombardment at the inner wall surface.

- The metal temperature at the crack tip is sufficiently high to result in "upper shelf" or ductile behavior.

- The upper shelf toughness is sufficiently high to preclude low energy tearing. The latter process can proceed in a rapid or unstable manner at constant load.

If the stable crack extension is shown to be small compared with the remaining wall ligament, then the vessel integrity will be maintained. If correctly predicted, this behavior will preclude the melting of the reactor core that could have occurred due to the loss of cooling water through the fully-cracked wall. An experimental program was therefore undertaken to simulate the bending of the vessel wall and to characterize the nature of the crack extension.

EXPERIMENTAL INVESTIGATION

Experimental Procedure

The pure bending in the plastic net ligament of the vessel wall was simulated by the four-point bending of a cracked beam as illustrated in Fig. 16. Specimens were machined from A533-B steel plate (HSST plate 02) and were identical in all respects to the 38mm WPS specimens described in the previous section. As with the WPS experiments, a portion of the specimens was face grooved.

In accordance with the preceding requirements for ductile behavior, the tests were conducted within the upper shelf regime (approximately 93°C, 200°F) to assure a high level of fracture toughness. The specimens were heated in an oven to the required temperature and then placed in the same loading fixture used for the WPS experiments. The specimens were loaded slowly in four-point bending to various levels of mid span deflection. For comparison, some specimens were also subjected to three-point bending. The deflections of various specimens were controlled so as to impose bend angles both smaller and larger than the theoretical value of 2° computed for a typical vessel. During loading the specimen temperature decreased on the order of 10°C (18°F), but this decrease was insufficient to prevent the attainment of the upper shelf

toughness level throughout the test. The specimens were removed from the loading fixture and the plastic bend angle (θ) was determined optically from the position of the machined notch flanks. The specimens were then heat tinted to mark the crack extension and broken apart at a low temperature. Crack extension was measured with a traveling microscope and an average was obtained from measurements at the 1/4, 1/2 and 3/4 thickness positions.

Test Results

The experimental results for 38mm thick bend specimens are presented in Fig. 17. In spite of a large scatter exhibited by the data, it is clear that the crack extension is small, less than 7mm (0.28 in.), even for a bend angle of 4°; the latter is twice the bend angle predicted from a mathematical model[13]. The curve of bend angle vs crack extension in Fig. 17 exhibits proportionately more crack extension with each successive degree of bend angle. This trend is expected as the specimen achieves its limit load. In addition, the data exhibit no trends that can be attributed to three-point bend vs four-point bend nor to the presence or absence of face grooves.

In all cases the crack front extended first at the crack mid plane; this resulted in a tunneled shape that became more severe with increasing bend angle. Except for the specimen having a 4° bend angle, no crack extension on the surfaces was observed.

As might be expected with tests in the plastic regime, a slight lateral contraction was present at the notch root. For a 2° bend angle the notch root contraction was approximately 0.6mm (0.024 in.) on either side of the notch. It should be noted that the presence of face grooves did not appear to reduce the notch root contraction at a given bend angle.

DISCUSSION

Inspection of Fig. 17 leads to the conclusion that a plastic bend angle of approximately 2° will cause only a small crack extension, 3mm, in a bend specimen. In translating this observation to a typical vessel wall having a thickness of 216mm and an assumed crack depth of 173mm, it is apparent that a crack extension of 3mm in the remaining ligament would be negligible.

One must use caution in applying the experimental results directly to project the vessel behavior. This comparison is valid only if the crack-tip constraint is similar in both the specimen and the vessel wall. With respect to the constraint

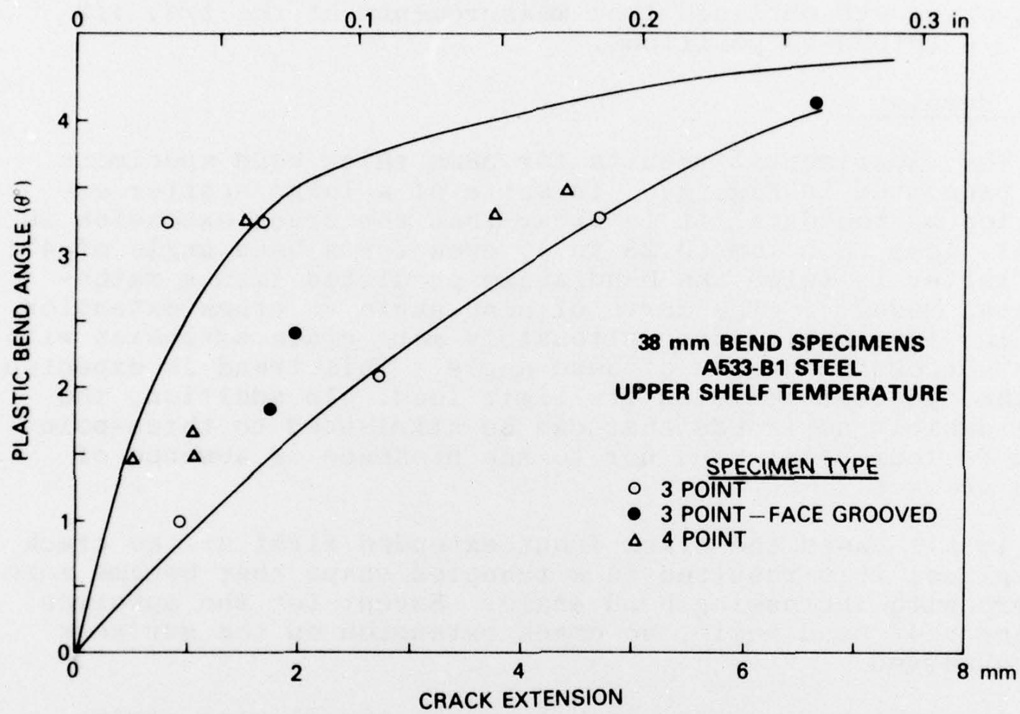

Fig. 17 — Ductile crack extension occurring in a bend specimen as a function of the imposed plastic bend angle

in the direction of crack propagation, both the vessel and specimen have the same net ligament (approximately 43mm) so that the constraint in both bodies is similar. However, due to the limited specimen thickness, the transverse constraint in the specimen is less than that in the vessel. In other words, the through-thickness yielding in the specimen must be prevented in order to achieve an accurate simulation of the vessel constraint. For a given bend angle one would expect a larger crack extension in the vessel wall because of its larger transverse constraint. Therefore, additional experiments are required to characterize the contribution of the specimen thickness to the crack extension at a fixed bend angle. The effect of thickness can be demonstrated simply by increasing the specimen thickness while retaining the planar dimensions.

From the present results it is felt that the yielding by both the specimen and vessel in the direction of crack propagation (i.e., plastic net ligament) will dominate the crack extension. Consequently, the crack extension trend in Fig.17 should reasonably approximate the actual extension in the vessel wall. However, follow-on experiments will be conducted with specimens of increased thickness, 76mm vs 38mm, to define the thickness-dependence of crack extension.

Finally, a comment is in order concerning the influence of the face grooves on the crack extension. Face grooves are believed to provide additional transverse constraint, such as would be associated with increased thickness. The results of the present investigation suggest that 5% face grooves do not provide additional transverse constraint. Specifically, the notch root contraction for both types of specimens was essentially identical. One would have expected a smaller notch root contraction if the face grooves had provided additional transferse constraint. The experimental results, illustrated in Fig. 17, show no effect of the face grooves, thereby supporting the above conclusion regarding their significance. However, it can be argued that face grooves of much greater depth could increase the constraint.

SUMMARY AND CONCLUSIONS

A simulation of the postulated plastic net ligament behavior during a LOCA was achieved by means of fatigue-cracked bend specimens. The specimens were loaded to a bend angle identical to that computed for the vessel wall. The experiments were restricted to the upper shelf or ductile toughness regime under the assumption that the material in the vicinity of a deep crack in a vessel wall would exhibit a similar toughness. Under these conditions, the bend specimens exhibited a negligible crack extension. On the

basis that the test specimens adequately simulate the constraint of a deep crack in the vessel wall, it is concluded that the crack in a vessel will extend a negligible amount as a result of the bending of the vessel wall caused by the thermal stresses. Consequently, the integrity of the wall will be maintained. However, the specimens do not exactly simulate the constraint of the vessel wall; additional experiments with specimens of increased thickness are required for a conclusive demonstration of the crack extension caused by the rotation of the vessel wall.

In the case of a highly embrittled wall, the resulting temperature elevation of the brittle-ductile transition may place the crack tip within the transition region rather than the upper shelf region. In this case the conclusions of the present study are not applicable. Furthermore, it should be noted that, within the transition region, unstable crack propagation can be exhibited by material that has been plastically deformed. In other works, a cleavage fracture mode has been observed after plastic deformation caused by <u>static</u> loading at a temperature below the upper shelf toughness regime, the latter being defined by a <u>dynamic</u> test. The cleavage fracture mode is absent only at temperatures that lie within the upper shelf regime. Therefore, the conclusions of the present study must be restricted to the upper shelf regime.

As a final consideration, it has been shown by Cheverton[14] that the critical K_{Ic} level can be achieved by the crack-tip region as the wall continues to cool during the LOCA. In this event one must rely on the phenomenon of WPS as the basis upon which to project continued vessel integrity.

III. FATIGUE CRACK PROPAGATION IN LWR MATERIALS

A. Evaluation of Critical Factors in Crack Growth Rate Studies

H. E. Watson, B. H. Menke, and F. J. Loss

BACKGROUND

Experimental results discussed here relate to an evaluation of the effects of water, temperature, and cycling rate on the fatigue crack propagation (FCP) in A508-2 forging material. Emphasis was placed on one material for the subject studies to minimize the effect of this variable on FCP. Tests are being conducted in accordance with a preliminary matrix developed by the Nuclear Regulatory Commission (NRC) to simulate (a) the hydro and leak transient, and (b) the heatup and cooldown transient of a commercial nuclear pressure vessel. The test conditions corresponding to these two conditions are, respectively, 93°C (200°F) water at atmospheric pressure and 288°C (550°F) water at a pressure of 14 MPa (2000 psi). Test specimens used in this series are 25mm (1 in.) thick compact tension (CT). The other test parameters included: a modified trapezoidal waveform with a rise time of 1 sec, an R-ratio of 0.1 and cyclic frequencies of 1, 0.33, and 0.08 cycles per minute (CPM). Crack length measurements are referenced to the crack mouth opening (CMO) and in all cases, the crack growth rate, da/dN, values were determined by computer analysis using the incremental polynominal technique recommended by the ASTM Task Group on Fatigue Crack Growth Rate Testing.[15]

EXPERIMENTAL PROCEDURE

The FCP data were generated using both autoclave and water pot fatigue test equipment to simulate the heatup and hydro transients, respectively. The autoclave is pressurized to 14 MPa (2000 psi) and heated to 288°C (550°F). The autoclave water is circulated through a filter and returned to a reservoir which is pressurized with hydrogen to 0.2 MPa (30 psi). This maintains the dissolved hydrogen at 30 to 50 cc/Kg in accordance with water specifications in a pressurized water reactor (PWR) system. Crack length measurements are referenced to the CMO. Measurements of the CMO are determined using a linear variable differential transformer (LVDT) designed to withstand the autoclave environment. LVDT measurements are then converted to crack lengths using compliance data obtained from A533-B steel specimens having machined notches of different depths.

The water pot is heated to 93°C (200°F) and water is circulated to insure uniform water chemistry. A blanket of nitrogen is provided under a slight pressure to stabilize the chemical composition of the water. CMO measurements, using a clip gage, are referenced to the crack length in the same manner as in the autoclave tests.

The water used in the autoclave and water pot apparatus simulates, as nearly as possible, the actual PWR water chemistry. Preliminary water specifications have been prepared after consultation with reactor vendors. The chemical composition is as follows:

oxygen	- 10 ppb (beginning of test)
	<10 ppb (remainder of test)
hydrogen	- 30 to 50 cc/Kg
conductivity	- <20 μmhos
boron	- control at 1000 ppm
	- allowable range of 500 to 1500 ppm
chloride	- <0.15 ppm
fluoride	- <0.15 ppm
lithium	- 0.2 to 2.0 ppm as LiOH. Control of the pH is maintained by the proper levels of boron and independent control is not specified.

RESULTS

Results are presented in Fig. 18 for duplicate tests in 93°C (200°F) water at 1 cpm. The modified trapezoidal wave form included a 1 sec up/down ramp. For comparison, data generated in an air environment at 288°C (550°F) with a modified trapezoidal wave form are also shown. Previous tests with A533-B and A508-2 steels in an air environment at 288°C have shown no difference between cycling rates of 0.1 and 10 cpm.[16] Both the water and the air data in Fig. 18 fall very close to the ASME Section XI upper boundary line for FCP in air. One may therefore conclude that the water environment does not cause a significant increase in FCP for the particular conditions investigated.

To evaluate the effect of varying the time at maximum load, tests were initiated using hold times of 3 and 12 minutes (0.3 and 0.08 cpm) in the water pot environment. Data from these tests and the 1 cpm data on Fig. 18 are shown in Fig. 19. A comparison of these data reveals that hold times of 1, 3 and 12 minutes produced no significant effect on the FCP for this test condition. One occurrence during the 3 min hold time test should be mentioned, however. This test exhibited a reduction in FCP rate near its beginning. Westinghouse Corp. has had a similar experience, with a

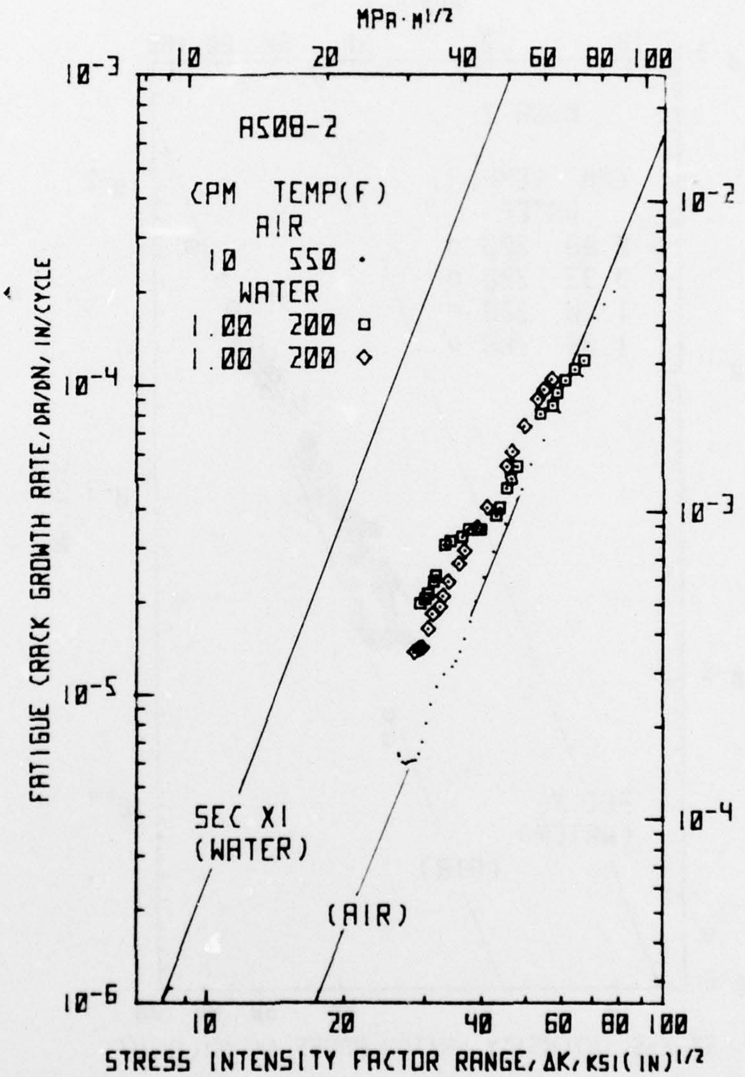

Fig. 18 — Comparison of FCP trends at 1 CPM in 93°C (200°F) water with 10 CPM data in air at 288°C (550°F). A modified trapezoidal waveform having a 1 sec rise time was used for all the tests.

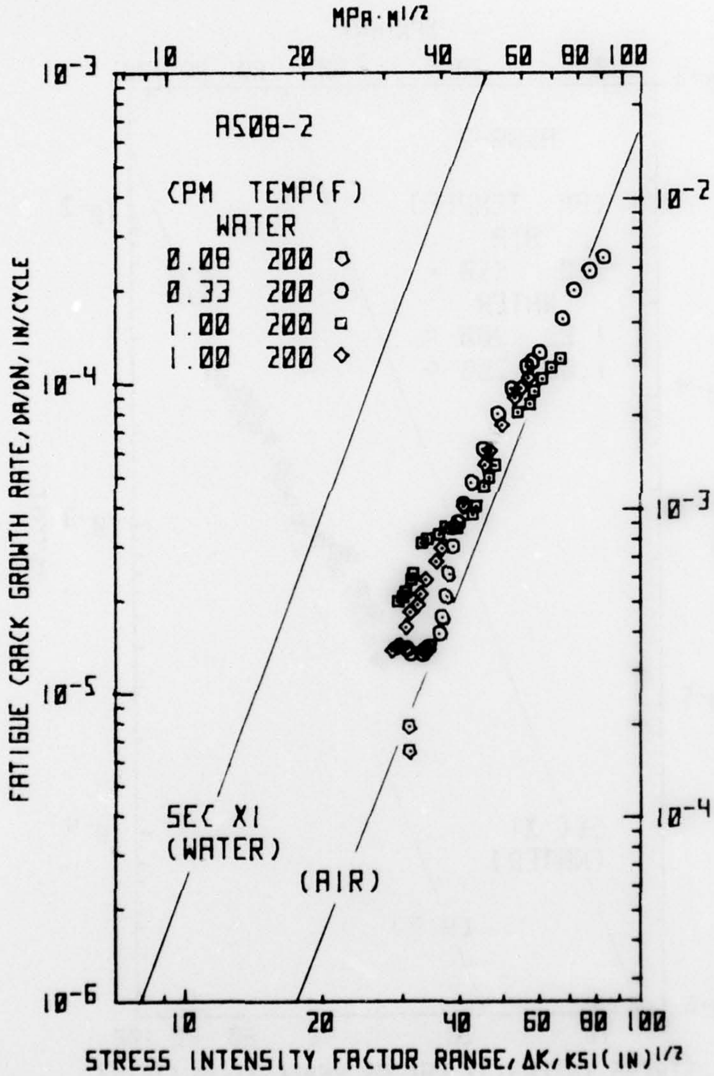

Fig. 19 — Comparison of the effect of hold time on FCP tests conducted in 93°C (200°F) water. All tests were subjected to a modified trapezoidal loading pattern having a 1 sec rise time.

decrease in FCP rate occurring after the test equipment had been shutdown for a period of time. An examination of the test record revealed that the reduction in FCP rate for this specimen occurred after the equipment had also been shut down. An investigation is being conducted to determine if a correlation exists between the reduction in crack growth rate and the shut-down occurrences.

Autoclave tests were completed on two specimens at 1 cpm to evaluate the effect of the higher temperature, 288°C (550°F) and pressure on FCP. These data (not illustrated) fall within the scatterband of the 93°C (200°F) data and suggest that the temperature and pressure increase have no effect on FCP for this material and these test conditions. One of these tests was shut down for a significant period on two occasions. Each event resulted in a period of reduced FCP. With each event, the data trend exhibited a perturbation so as to indicate a lower crack growth rate for a given value of ΔK. Therefore, to prevent introducing other variables into the test matrix, it will be essential that the tests not be interrupted.

CONCLUSIONS

The present data suggest that, for the A508-2 f..ging and a rapid loading rate, there is no significant effect of hold time, temperature, pressure, or water environment on FCP in a PWR environment.

REFERENCES

1. U. Potapovs and J. R. Hawthorne, "The Effect of Residual Elements on 550°F Irradiation Response of Selected Pressure Vessel Steels and Weldments," NRL Report 6803, Naval Research Laboratory, 22 Nov 1968.

2. J. R. Hawthorne, "Demonstration of Improved Radiation Embrittlement Resistance of A533-B Steel Through Control of Selected Residual Elements," NRL Report 7121, Naval Research Laboratory, 21 May 1970; and ASTM STP 484, 1971, 96-126.

3. J. R. Hawthorne, "Radiation Resistant Weld Metal for Fabricating A533-B Nuclear Reactor Vessels," Welding Journal Research Supplement, Vol. 51, No. 7, July 1972, 369s-375s.

4. J. R. Hawthorne, J. J. Koziol and R. D. Groeschel, "Evaluation of Commercial Production A533-B Plates and Weld Deposits Tailored for Improved Radiation Embrittlement Resistance," ASTM STP 570,1976, 83-102.

5. J. R. Hawthorne, E. Fortner, and S. P. Grant, "Radiation Resistant Experimental Weld Metals for Advanced Reactor Vessel Steels," Welding Journal Research Supplement, Vol. 49, No. 10, October 1970, 453s.

6. E. C. Biemiller and S. T. Byrnes, "Evaluation of the Effect of Chemical Composition on the Irradiation Sensitivity of Reactor Vessel Weld Metal," ASTM STP 611, 1976, 418-433.

7. F. J. Loss, Editor,"Structural Integrity of Water Reactor Pressure Boundary Components, Progress Report Ending 31 May 1976," NRL Memorandum Report 3353, NRL NUREG 2, Naval Research Laboratory, September 1976.

8. F. A. Smidt, Jr. and J. A. Sprague, "Properties Changes Resulting from Impurity-Defect Interactions in Iron and Pressure Vessel Steel Alloys," ASTM STP 529, 1973, pp. 78-91.

9. W. O. Shabbits, "Dynamic Fracture Properties of Heavy Section A533-Grade B Class 1 Steel Plate," WCAP-7623, Heavy Section Steel Technology Program Technical Report No. 13, Westinghouse Research and Development Center, Pittsburgh, PA, Dec 1970.

10. W. O. Shabbits, W. H. Pryle, and E. T. Wessel, "Heavy Section Fracture Toughness Properties of A533 Grade B, Class 1 Steel Plate and Submerged Arc Weldment," WCAP-7414, Heavy Section Steel Technology Program, Technical Report No. 6, Westinghouse Research and Development Center, Pittsburgh, PA, Dec 1969.

11. R. D. Cheverton, "Pressure Vessel Fracture Studies Pertaining to a PWR LOCA-ECC Thermal Shock: Experiments TSE-1 and TSE-2", ORNL/NUREG/TM-31, Oak Ridge National Laboratory, Oak Ridge, TN, Sep 1976.

12. "Effects of Residual Elements on the Predicted Radiation Damage to Reactor Vessel Materials," Regulatory Guide 1.99, U. S. Nuclear Regulatory Commission, Office of Standards Development.

13. J. G. Merkle, unpublished, Oak Ridge National Laboratory, Oak Ridge, TN.

14. R. D. Cheverton, unpublished, Oak Ridge National Laboratory, Oak Ridge, TN.

15. W. G. Clark, Jr., and S. J. Hudak, Jr., "Variability in Fatigue Crack Growth Rate Testing," Scientific Paper No. 74-1E7-MSLRA-P2, Westinghouse Research Laboratories, Pittsburgh, PA., Sep 18, 1974.

16. F. J. Loss, Editor, "Structural Integrity of Water Reactor Pressure Boundary Components, Progress Report Ending 29 February 1976," NRL Report 8006, NRL NUREG 1, Aug 26, 1976.